https://doi.org/10.5194/acp-2020-1190
Preprint. Discussion started: 11 December 2020


Atmospheric Chemistry and Physics Discussions

# Estimates of mass absorption cross sections of black carbon for filter-based absorption photometers in the Arctic

Sho Ohata[1,2,*], Tatsuhiro Mori[3,*], Yutaka Kondo[4,*], Sangeeta Sharma[5], Antti Hyvärinen[6], Elisabeth Andrews[7,8], Peter Tunved[9], Eija Asmi[6], John Backman[6], Henri Servomaa[6], Daniel Veber[5], Makoto Koike[10], Yugo Kanaya[11,12], Atsushi Yoshida[10], Nobuhiro Moteki[10], Yongjing Zhao[13], Junji Matsushita[4], and Naga Oshima[14]

[1]Institute for Space–Earth Environmental Research, Nagoya University, Nagoya, Aichi, Japan
[2]Institute for Advanced Research, Nagoya University, Nagoya, Aichi, Japan
[3]Department of Physics, Faculty of Science Division I, Tokyo University of Science, Tokyo, Japan
[4]National Institute of Polar Research, Tokyo, Japan
[5]Climate Chemistry Measurements Research/Climate Research Division, Environment and Climate Change Canada/Government of Canada
[6]Finnish Meteorological Institute, Helsinki, Finland
[7]Cooperative Institute for Research in Environmental Sciences (CIRES), University of Colorado, Boulder, CO, USA
[8]NOAA Global Monitoring Laboratory, 325 Broadway, Boulder, CO, USA
[9]Department of Environmental Science and Analytical Chemistry (ACES), Atmospheric Science Unit, Stockholm University, Stockholm, Sweden
[10]Department of Earth and Planetary Science, Graduate School of Science, The University of Tokyo, Tokyo, Japan
[11]Research Institute for Global Change (RIGC), Japan Agency for Marine-Earth Science and Technology (JAMSTEC), Yokohama, Kanagawa, Japan
[12]Graduate School of Maritime Sciences, Kobe University, Kobe, Japan
[13]Air Quality Research Center, University of California, Davis, CA, USA
[14]Meteorological Research Institute, Tsukuba, Japan

[*]These authors contributed equally to this work.

*Correspondence to*: Sho Ohata (sho.ohata@isee.nagoya-u.ac.jp)

https://doi.org/10.5194/acp-2020-1190
Preprint. Discussion started: 11 December 2020


Atmospheric Chemistry and Physics
Discussions

**Abstract.** Long-term measurements of black carbon (BC) are warranted for investigating changes in its emission, transport, and deposition. However, depending on instrumentation, parameters related to BC such as aerosol absorption coefficient ($b_{abs}$) have been measured instead. Most ground-based measurements of $b_{abs}$ in the Arctic have been made by filter-based absorption photometers, including multi-angle absorption photometers (MAAP), particle soot absorption photometers (PSAP), continuous light absorption photometer (CLAP), and Aethalometers. The measured $b_{abs}$ can be converted to atmospheric mass concentrations of BC ($M_{BC}$) by assuming the value of the mass absorption cross section (MAC = $b_{abs}/M_{BC}$). However, the accuracy of conversion of $b_{abs}$ to $M_{BC}$ has not been adequately assessed. Here, we introduce a systematic method for deriving MAC values from $b_{abs}$ measured by these instruments and independently measured $M_{BC}$. In this method, $M_{BC}$ was measured with a filter-based absorption photometer with a heated inlet (COSMOS). COSMOS-derived $M_{BC}$ ($M_{BC}$ (COSMOS)) is traceable to a rigorously calibrated single particle soot photometer (SP2) and the absolute accuracy of $M_{BC}$ (COSMOS) has been demonstrated previously to be about 15 % in Asia and the Arctic. The necessary conditions for application of this method are a high correlation of the measured $b_{abs}$ with independently measured $M_{BC}$, and long-term stability of the correlation slope, which represents the MAC. In general, $b_{abs}$ - $M_{BC}$ (COSMOS) correlations were high ($r^2$ = 0.84–0.96 for hourly data) at Fukue in Japan, Barrow in Alaska, Ny-Ålesund in Svalbard, Pallastunturi in Finland, and Alert in Canada, and stable up to for 10 years. We successfully estimated MAC values (11.0–15.2 m$^2$ g$^{-1}$ at a wavelength of 550 nm) for these instruments and these MAC values can be used to obtain error-constrained estimates of $M_{BC}$ from $b_{abs}$ measured at these sites even in the past, when COSMOS measurements were not made. Because the absolute values of $M_{BC}$ in these Arctic sites estimated by this method are consistent with each other, they are applicable to study spatial and temporal variation of $M_{BC}$ and to evaluate performance of numerical model calculations.

https://doi.org/10.5194/acp-2020-1190
Preprint. Discussion started: 11 December 2020


Atmospheric Chemistry and Physics
Discussions

## 1 Introduction

Black carbon (BC) particles strongly absorb solar radiation and therefore impact the radiation budget in the Arctic (Bond et al., 2013; Arctic Monitoring and Assessment Programme (AMAP), 2015). In addition, BC deposited on snow decreases the snow surface albedo and accelerates snowmelt (AMAP, 2015; Flanner et al., 2009). According to recent climate model calculations in the sixth phase of the Coupled Model Intercomparison Project (CMIP6; Eyring et al., 2016), BC provides the second largest contribution to the positive radiative forcings in the Arctic after carbon dioxide ($CO_2$) (Oshima et al., 2020). BC is one of the short-lived climate forcers (SLCF) and reductions of BC emissions can decrease the positive Arctic radiative forcing over much shorter timescales than reductions of $CO_2$ emissions (Sand et al., 2016). Long-term measurements of mass concentrations of BC in the atmosphere ($M_{BC}$) at various locations provide fundamental data for the detection of long-term trends in $M_{BC}$ in the Arctic that are associated with changes in BC emissions. Such $M_{BC}$ data are also useful for validation and improvement of climate models. However, because many long-term surface instruments measure aerosol light absorption coefficient ($b_{abs}$) rather than $M_{BC}$, there are large uncertainties in $M_{BC}$ estimated from the measurements of $b_{abs}$ that have not been critically evaluated.

A continuous soot monitoring system called COSMOS (Kanomax, Osaka, Japan) has been developed to measure $M_{BC}$ (Miyazaki et al., 2008; Kondo et al., 2009, 2011). This filter-based absorption photometer is equipped with an inlet that is heated to 300°C to remove non-refractory components from the aerosol phase. Comparisons of the $M_{BC}$ values measured by COSMOS ($M_{BC}$ (COSMOS)) with those measured by a single particle soot photometer (SP2; Droplet Measurement Technologies, Longmount, CO, USA; $M_{BC}$ (SP2)), which is based on a laser-induced incandescence technique (Schwarz et al., 2006; Moteki and Kondo, 2010), in Asia and at Ny-Ålesund in Svalbard (Kondo et al., 2009, 2011; Ohata et al., 2019) have shown that $M_{BC}$ (SP2) and $M_{BC}$ (COSMOS) agree to within about 10%.

Other types of filter-based absorption photometers, including the multi-angle absorption photometers (MAAP; Thermo Scientific, Waltham, MA, USA), particle absorption soot photometers (PSAP; Radiance Research, Seattle, WA, USA), continuous light absorption photometer (CLAP; NOAA, Boulder, CO, USA; Ogren et al., 2017) and Aethalometers (Magee Scientific, Berkeley, CA, USA) have been used for long-term measurements of $b_{abs}$ at various sites. However, as the measurements of $b_{abs}$ by these instruments are known to be affected both by measurement artefacts (i.e. the scattering effect, e.g. Bond et al., 1999) and enhanced absorption due to the lensing effect (Bond et al., 2006), the accuracy and stability of conversion of $b_{abs}$ obtained by these instruments to $M_{BC}$ have not yet been fully evaluated. Evaluations that have been completed to date include those of Kanaya et al. (2013, 2020), who compared $M_{BC}$ (COSMOS) with the $b_{abs}$ measured by MAAP ($b_{abs}$ (MAAP)) on Fukue Island,

https://doi.org/10.5194/acp-2020-1190
Preprint. Discussion started: 11 December 2020




Japan (32.8°N, 128.7°E), and Sinha et al. (2017), who compared $b_{abs}$ measured by PSAP ($b_{abs}$ (PSAP)) at Barrow in Alaska (71.3°N, 156.6°W) and Ny-Ålesund in Spitsbergen (78.9°N, 11.9°E) (Fig. 1). The results of these studies showed that $b_{abs}$ (MAAP) and $b_{abs}$ (PSAP) were strongly correlated with $M_{BC}$ (COSMOS), making it possible to convert $b_{abs}$ to $M_{BC}$ at these sites with reasonable accuracy.

Long-term observations of $b_{abs}$ have been made also at Pallastunturi in Finland (68.0°N, 24.0°E) by MAAP (Hyvärinen et al., 2011; Lihavainen et al., 2015) and at Alert in Canada (82.5°N, 62.5°W) by PSAP and Aethalometer (Sharma et al., 2004, 2006, 2017). To investigate the possibility of converting $b_{abs}$ to $M_{BC}$ at each of these sites, it is important to simultaneously measure $M_{BC}$ and $b_{abs}$ by collocating a COSMOS (or SP2) at each site with each of these filter-based absorption photometer instruments.

In this paper, we critically re-examine the concepts underpinning the use of filter-based instruments to estimate $M_{BC}$. We derive mass absorption cross sections (MAC) for MAAP, PSAP/CLAP, and Aethalometer measurements based on their comparison with COSMOS measurements. We also analyze the variability of the MACs derived and their dependencies on instrument type and observation site.

## 2 Methods

### 2.1 SP2

In this study we used the SP2 and COSMOS as standard instruments to measure $M_{BC}$. Detailed descriptions of the SP2, including calibration methods, are given elsewhere (Schwarz et al., 2006; Moteki and Kondo, 2010). In short, the SP2 uses the laser-induced incandescence technique and detects BC on a single-particle basis. We used two SP2s in this study: one was installed at Fukue and maintained and calibrated by the University of Tokyo (UT-SP2, hereafter) and the other one at Alert maintained and calibrated by Environmental and Climate Change Canada (EC-SP2, hereafter). The configuration of the UT-SP2 is identical to that described by Moteki and Kondo (2010). The manufacturer's model version of the EC-SP2 is "SP2-D" with eight channels. The UT-SP2 and EC-SP2 measured BC size distributions in the mass-equivalent diameter ($D_m$) range 70–850 nm and 60–600 nm, respectively. The void-free density of BC was assumed to be 1.8 g cm$^{-3}$. These SP2s were calibrated using fullerene soot particles (Moteki and Kondo, 2010, Kondo et al., 2011). The laser-induced incandescence signal intensity of the UT-SP2 for the specific mass of ambient BC particles in Tokyo agreed with that of fullerene soot particles to within about 10% (Kondo et al., 2011). Laborde et al. (2012) reported similar SP2 calibration curves for fullerene soot particles, diesel exhaust, and ambient BC particles in Switzerland. The accuracy of $M_{BC}$ (SP2) estimated from the uncertainty of the calibration and operational conditions of SP2 was about 10%. No particle-size cut was used for the inlet of the UT-SP2, whereas a $PM_1$ cyclone was used for the EC-SP2.

https://doi.org/10.5194/acp-2020-1190
Preprint. Discussion started: 11 December 2020



## 2.2 COSMOS

### 2.2.1 Accuracy of $M_{BC}$ measured by COSMOS

The principles of operation of the COSMOS apparatus are detailed in previous papers (Miyazaki et al., 2008; Kondo et al., 2011; Kondo, 2015; Ohata et al., 2019). Briefly, the COSMOS measures the extinction coefficient ($b_0$) of aerosols collected on a quartz-fiber filter at a given wavelength ($\lambda$ = 565 nm). Most previous studies used filters from Pallflex (E70-2075W, Pall, USA), which are no longer available. Consequently, HEPA filters have been used for more recent observations (Irwin et al., 2015), including this study. Because the COSMOS inlet is heated to 300°C, the effect on $b_0$ of light extinction by volatile light scattering particles (LSPs) can be ignored. The COSMOS is equipped with a $PM_1$ cyclone to minimize the effect of refractory non-BC particles in coarse mode, such as dust and sea-salt particles. Therefore, the absorption coefficient of BC for COSMOS [$m^{-1}$] is given as

$$b_{\text{abs}}\,(\text{COSMOS}) = f_{\text{fil}} b_0. \tag{1}$$

Here, $f_{\text{fil}}$ is a factor used to correct for the increase of absorption caused by multiple scattering in the filter medium (Bond et al., 1999; Ogren, 2010; Ohata et al., 2019). The MAC for the COSMOS [$m^2\ g^{-1}$] is operationally defined as

$$\text{MAC}\,(\text{COSMOS, SP2}) \equiv \frac{b_{\text{abs}}\,(\text{COSMOS})}{M_{\text{BC}}\,(\text{SP2})}, \tag{2}$$

where the numerator and denominator, respectively, are simultaneous measurements of $b_{\text{abs}}$ [$m^{-1}$] by COSMOS and BC mass concentration [$g\ m^{-3}$] of ambient air measured by SP2. The MAC value for a Pallflex filter at $\lambda$ = 565 nm was previously set at 8.73 [$m^2\ g^{-1}$] (Sinha et al., 2017). For a HEPA filter, the MAC is about 6% higher (Irwin et al., 2015).

Once the MAC (COSMOS, SP2) is determined, $M_{\text{BC}}$ (COSMOS) [$g\ m^{-3}$] at standard temperature and pressure (0°C, 1013 hPa) can be estimated as

$$M_{\text{BC}}\,(\text{COSMOS}) = \frac{b_{\text{abs}}\,(\text{COSMOS})}{\text{MAC}\,(\text{COSMOS,SP2})}. \tag{3}$$

If for some reason $b_{\text{abs}}$ (COSMOS) is changed by a constant factor α, for example by changes in the correction factor $f_{\text{fil}}$ or the type of the filter used, we denote this new $b_{\text{abs}}$ (COSMOS) value as $b_{\text{abs}}^{\alpha}$ (COSMOS) = α × $b_{\text{abs}}$ (COSMOS). Then, the corresponding MAC (COSMOS, SP2) is calculated as MAC (COSMOS, SP2)$^{\alpha}$ = $\alpha$ × MAC (COSMOS, SP2), according to Eq. (2) by comparison of $b_{\text{abs}}^{\alpha}$ (COSMOS) and $M_{\text{BC}}$ (SP2). However, the factor α for each of $b_{\text{abs}}^{\alpha}$ (COSMOS) and MAC$^{\alpha}$ cancels out in the calculation of $M_{\text{BC}}^{\alpha}$(COSMOS).

We call the COSMOS that was calibrated by comparison with the SP2 in Tokyo the "standard COSMOS", described hereafter as Std-COSMOS. Because the MAC of the Std-COSMOS was determined by comparison with SP2 (Eq. (2)), it acts as a transfer standard for the SP2. The $b_{\text{abs}}$

https://doi.org/10.5194/acp-2020-1190
Preprint. Discussion started: 11 December 2020


Atmospheric Chemistry and Physics Discussions

(COSMOS) of each COSMOS manufactured is compared with the Std-COSMOS by sampling ambient BC particles in Osaka, Japan, typically for 1–2 weeks. The comparisons during these periods were statistically reliable partly due to relatively high BC concentrations in Osaka. The $b_{abs}$ (COSMOS) of 28 COSMOS instruments manufactured thus far agreed with that of Std-COSMOS to within about ±7%, indicating reliable quality control in manufacturing. The small differences originating from the uncertainty of the filter sampling spot size of each unit are corrected for in deriving $M_{BC}$ (COSMOS).

It is important to compare $M_{BC}$ (COSMOS) and $M_{BC}$ (SP2) outside Tokyo and Osaka, to confirm both the strong correlation between $M_{BC}$ (COSMOS) and $M_{BC}$ (SP2) and the long-term stability of $M_{BC}$ (COSMOS) value. Ohata et al. (2019) made these comparisons at two remote sites: at Cape Hedo (26.9°N, 128.3°E), Japan, and at Ny-Ålesund. At each of these locations, the concentrations of BC and LSP and the mixing states of BC were considerably different from those in Tokyo and Osaka. $M_{BC}$ (COSMOS) and $M_{BC}$ (SP2) agreed to within about 10% at these sites, thus demonstrating the validity of using the Std-COSMOS to calibrate each of the COSMOS instruments to be used for field observations. Ohata et al. (2019) also showed that the dependencies of MAC (COSMOS) on the thickness of coatings of BC particles, $M_{BC}$, and volume concentrations of the co-existing LSPs were small. Although the MAC (COSMOS) showed a slight dependence on the mass size distributions of BC, the sensitivity of the MAC (COSMOS) to such variations in microphysical properties of BC was generally less than 10% (Kondo et al., 2011; Ohata et al., 2019).

Previously estimated uncertainties of $M_{BC}$ (COSMOS) were about 10% based on the range of agreement between $M_{BC}$ measurements by COSMOS and SP2 (Kondo et al., 2011; Ohata et al., 2019). It may be more appropriate to estimate the absolute accuracy of $M_{BC}$ (COSMOS) to be about 15%, including the above-mentioned 10% uncertainty of $M_{BC}$ (SP2).

### 2.2.2 Effect of light-absorbing $FeO_x$ particles on $M_{BC}$

Light-absorbing iron oxide ($FeO_x$) aerosols, which the SP2 can distinguish from BC (Yoshida et al., 2016; Lamb, 2019), can affect $M_{BC}$ measured by filter-based absorption photometers. $FeO_x$ aerosols are emitted from both anthropogenic sources (e.g., motor vehicle exhaust) and natural sources (e.g., wind-blown mineral dust). Within the detectable diameter range of the UT-SP2 ($D_m$ = 70–850 nm for BC and $D_m$ =170–2100 nm for $FeO_x$), the mass concentration ratios of $FeO_x$ to BC were typically ~0.4 in East Asia and ~0.2 in the Arctic; they were mainly of anthropogenic origin in both regions (Moteki et al., 2017; Ohata et al., 2018; Yoshida et al., 2018, 2020). $FeO_x$ aerosols contribute at least 4–7% of the short-wave absorbing powers of BC in Asian continental outflows (Moteki et al., 2017) and their direct radiative forcing has been estimated to be 0.22 W $m^{-2}$ over East Asia (Matsui et al., 2018). Here, we estimate the effect of light absorption by $FeO_x$ on $M_{BC}$ measured by the COSMOS. The ratio of light absorbed by $FeO_x$ to that absorbed by BC at a wavelength $\lambda$ ($\varepsilon(\lambda)$) is given by

https://doi.org/10.5194/acp-2020-1190
Preprint. Discussion started: 11 December 2020

Atmospheric Chemistry and Physics Discussions

$$\varepsilon(\lambda) = \frac{\int_{D_L}^{D_U} \frac{dM_{FeOx}}{d\log D_m} MAC_{Mie\_FeOx}(D_m,\lambda)\, d\log D_m}{\int_{D_L}^{D_U} \frac{dM_{BC}}{d\log D_m} MAC_{Mie\_BC}(D_m,\lambda)\, d\log D_m}, \quad (5)$$

where $D_m$ is mass equivalent diameter; $D_L$ and $D_U$ are the lower and upper limits, respectively, of the diameter for the integral calculus; $dM_{BC}/d\log D_m$ and $dM_{FeOx}/d\log D_m$ are the mass size distributions of BC and $FeO_x$, respectively; $MAC_{Mie\_BC}(D_m, \lambda)$ and $MAC_{Mie\_FeOx}(D_m, \lambda)$ are the MAC values of BC and $FeO_x$, respectively, for $D_m$ and $\lambda$ calculated by Mie theory.

The mass size distributions of BC and $FeO_x$ at Fukue and Ny-Ålesund (Fig. 2) were obtained by fitting monomodal and bimodal lognormal functions to the average mass size distributions measured by the SP2 during each observation campaign (Yoshida et al., 2020). The measurements at Fukue were made in April 2019 and those at Ny-Ålesund in March 2017. The $MAC_{Mie\_BC}(D_m, \lambda)$ and $MAC_{Mie\_FeOx}(D_m, \lambda)$ data (Fig. 2) were calculated by Mie theory for $\lambda = 565$ nm (wavelength used for COSMOS). For this calculation, we assumed BC and $FeO_x$ to be in the form of bare spheres with void-free densities of 1.80 g $cm^{-3}$ and 5.17 g $cm^{-3}$, respectively. The refractive index of BC we used was $1.99 + 0.64i$, which is the value for BC at $\lambda = 600$ nm (Bergstrom, 1972). The refractive index of $FeO_x$ we used was $2.56 + 0.57i$, which is the value for magnetite at $\lambda = 600$ nm (Huffman and Stapp, 1973).

From Eq. (5), the $\varepsilon$ values at Fukue and Ny-Ålesund were calculated to be 3.6% and 1.9%, respectively, for ($D_L$, $D_U$) = (30 nm, 1000 nm). These $\varepsilon$ values became 4.6% and 2.6% for ($D_L$, $D_U$) = (30 nm, 2500 nm). Because COSMOS is equipped with a $PM_1$ cyclone, we estimated the effect of light absorption by $FeO_x$ on $M_{BC}$ measured by COSMOS to be < 4% in East Asia and < 2% the Arctic. Note that these estimates are upper limits of the effect of $FeO_x$ because the $PM_1$ cyclone is designed to remove particles of > 1 μm aerodynamic diameter ($D_a$). Due to the fractal shape and high density of $FeO_x$ particles (Moteki et al., 2017), $D_m$ is considerably smaller than $D_a$ for $FeO_x$ particles and thus $D_U$ in Eq. (5) should be less than 1 μm.

The effect of $FeO_x$ on $M_{BC}$ (COSMOS) should be even smaller considering that the mass concentration of anthropogenic $FeO_x$ is correlated with $M_{BC}$, as mentioned above. Even if $b_{abs}$ (COSMOS) is enhanced by $FeO_x$ by a few percent, this effect is already incorporated to some extent, by operationally defining MAC (COSMOS, SP2) by Eq. (2).

The effect of $FeO_x$ on $b_{abs}$ may be somewhat higher for the other filter-based absorption photometers than for COSMOS if they are equipped with a larger particle size cut ($PM_{2.5}$ or $PM_{10}$). For accurate measurements of $M_{BC}$, the use of a $PM_1$ cyclone or impactor is recommended to minimize the effects of $FeO_x$, as well as other refractory particles such as natural dust and sea-salt particles.

https://doi.org/10.5194/acp-2020-1190
Preprint. Discussion started: 11 December 2020




### 2.3 Filter-based absorption photometers other than COSMOS

#### 2.3.1 MAAP

Detailed descriptions of the MAAP are given elsewhere (Petzold et al., 2002, 2005; Petzold and Schönlinner, 2004; Kanaya et al., 2013). In brief, the MAAP monitors the transmittance of light through a glass-fiber tape and measures reflectance at two angles. To remove the influence of LSPs, $b_{abs}$ (MAAP) from particles deposited on the filter is derived by radiative transfer calculations. The uncertainty of $b_{abs}$ (MAAP) was estimated by Petzold and Schönlinner (2004) to be 12%. The unit-to-unit variation of the MAAP was reported to be within 5% (Müller et al., 2011). The MAC values for the MAAP (MAC (MAAP)) for λ = 637 nm was determined by comparing $b_{abs}$ (MAAP) and $M_{BC}$ measured at four sites in Germany by the German reference method VDI2465 Part 1 (GRM; Schmid et al., 2001), represented by

$$\mathrm{MAC\ (MAAP, GRM)} \equiv \frac{b_{\mathrm{abs}}\,(\mathrm{MAAP})}{M_{\mathrm{BC}}\,(\mathrm{GRM})}. \quad (6)$$

For the measurements of $M_{BC}$ (GRM), organic carbons are removed by solvent extraction and the residual BC particles on filters were oxidized to $CO_2$, and quantified by coulometric titration. The measurement uncertainty of $M_{BC}$ (GRM) was about 25% (Petzold and Schönlinner, 2004). The MAC of 6.6 $m^2\ g^{-1}$ is recommended by the manufacturer based on their study. In determining MAC (MAAP, GRM), an SP2 was not used to measure $M_{BC}$, and this is a potential source of discrepancy in this value of MAC, as discussed in Sect. 3.2.

#### 2.3.2 PSAP and CLAP

The principle of operation of the PSAP is similar to those of COSMOS (Bond et al., 1999; Sinha et al., 2017). In this study, we also used $b_{abs}$ data obtained with a continuous light absorption photometer (CLAP) (Ogren et al., 2017). The CLAP is conceptually similar to the PSAP but uses a solenoid valve to cycle through eight sample filter spots. The PSAP and CLAP both utilize the Pallflex filters. The unit-to-unit variations of PSAP and CLAP were reported to be within 6% (Bond et al.,1999) and 4% (Ogren et al., 2017), respectively. The wavelengths of the light absorption measured by either PSAP or CLAP at Barrow, Ny-Ålesund, and Alert were about 467, 530, and 660 nm. The major difference of PSAP and CLAP from COSMOS is that sample air inlets of PSAP and CLAP are not heated to 300°C. Therefore, the effect of the attenuation of light by LSPs is corrected for by using the aerosol light scattering coefficient simultaneously measured by an integrating nephelometer (Bond et al., 1999; Ogren 2010). This correction adjusts for measurement artifacts but introduces uncertainties in the estimate of $b_{abs}$ (PSAP or CLAP). At the above three sites, light scattering coefficients measured by nephelometers at wavelengths of 450, 550, and 700 nm were used for this correction. The $b_{abs}$ for the PSAP or CLAP (hereafter, $b_{abs}$ (PSAP/CLAP)) at λ = 550 nm was obtained by adjusting measured absorption at 530 to 550 nm by using the $\lambda^{-1}$ relationship (Sinha et al., 2017; Sharma et al., 2017).

https://doi.org/10.5194/acp-2020-1190
Preprint. Discussion started: 11 December 2020



Schmeisser et al. (2017) reported that the median value of absorption Ångström exponent at Arctic sites was 1.04, which supports our assumption of the $\lambda^{-1}$ relationship.

### 2.3.3 Aethalometer

An AE-31 Aethalometer (Hansen et al., 1984) has been used for measurements of $b_{abs}$ at Alert (Sharma et al., 2017). This Aethalometer measures the attenuation of light transmitted through particles accumulating on a quartz fiber filter at seven wavelengths (370, 470, 520, 590, 660, 880, and 950 nm). In deriving $b_{abs}$ (Aethalometer) from attenuation data, the correction factor $C_f$ = 3.45 (Backman et al. (2017) was applied. This correction factor is very close to the correction factor $C_0$ = 3.5 recommended by World Meteorological Organization/Global Atmosphere Watch (2016). The direct corrections for the effects of aerosol loading artifact and light scattering by LSPs using nephelometer data were not applied for Aethalometer, which differs from the correction procedure for the PSAP/CLAP.

## 2.4 Interpretation of $b_{abs}$

The absorption coefficient of airborne BC particles ($B_{abs}$) [$m^{-1}$] is defined according to the Beer-Lambert law as

$$B_{abs}(\lambda) = \int C_{abs}(D_{BC}, \lambda) \frac{dN_{BC}}{d\log D_{BC}} d\log D_{BC}, \tag{7}$$

where $C_{abs}$ ($D_{BC}$, $\lambda$) [$m^2$] is the absorption cross section per airborne particle at wavelength $\lambda$ and depends not only on the diameter of BC particles ($D_{BC}$), but also on other parameters, such as coating thickness surrounding the BC particle that enhances light absorption (lens effect). $dN_{BC}/d\log D_{BC}$ is the number size distribution of BC. This $B_{abs}$ is different from $b_{abs}$ for the same ensemble of BC particles. The absorption coefficient of BC particles measured by filter-based absorption photometers ($b_{abs}$) is corrected for the effects of LSPs, as mentioned in Sections 2.2 and 2.3. The correction also accounts for multiple scattering within the filter material, where BC particles are embedded (Bond et al., 1999; Kondo, 2015) where the degree of amplification depends on filter materials. In addition, the magnitude of the lens effect may not be the same as for airborne BC particles because the coating on the BC particles may interact with the filter matrix (e.g., Lack et al., 2008). Thus, the correction algorithm applied to the filter-based light absorption photometer can lead to uncertainty in $b_{abs}$. Ogren et al. (2017) presents a detailed look at uncertainty in $b_{abs}$ for the CLAP (and by extension the PSAP). In practice, it is very difficult to estimate the uncertainty under different conditions of variables such as LSP/BC ratios, fractions of different types of LSPs with different optical properties (e.g., refractive indices), and the mixing state of BC. In this regard, $b_{abs}$ has often been erroneously assumed to represent $B_{abs}$ ($\lambda$).

In this paper, we focus on deriving $M_{BC}$ from $b_{abs}$, but taking into consideration the ambiguity of the physical definition of $b_{abs}$. We investigate the correlation of $b_{abs}$ with $M_{BC}$ directly measured and independent of $b_{abs}$. The conversion of $b_{abs}$ to $M_{BC}$ is possible when $b_{abs}$ is highly correlated with the measured $M_{BC}$ for sufficiently long periods. In that case, the $b_{abs}$ can be converted to $M_{BC}$ using the MAC (i.e., the slope of the $b_{abs}$ - $M_{BC}$ relationship). Note that MAC derived in this manner differs from MAC derived for airborne BC particles, as discussed above. Below, we show that MAC depends on the type of filter-based instrument and the locations where they are used.

## 3 Results and discussion

### 3.1 COSMOS–SP2 comparison

#### 3.1.1 Fukue

We used the UT-SP2 at Fukue for 3 weeks in April 2019 (Yoshida et al., 2020), as mentioned in Sect. 2.1. Fig. 3a shows the number and mass size distributions of BC measured by the UT-SP2 averaged over the observation period. In addition to the $M_{BC}$ (SP2) derived by integrating the mass size distributions over the detectable diameter range ($D_m$ = 70–850 nm), we also estimated $M_{BC}$ (SP2) in the $D_m$ = 30–1000 nm range by fitting a lognormal function to the data. As the two sets of $M_{BC}$ (SP2) values deviated by less than 2%, we used the former $M_{BC}$ (SP2) for comparison with $M_{BC}$ (COSMOS). The time series of hourly values of $M_{BC}$ (COSMOS) and $M_{BC}$ (SP2) (Fig. 3b) were strongly correlated ($r^2$ = 0.97) and the slope of the correlation was 0.92 (Fig. 3c). This relationship agrees with those observed by Ohata et al. (2019) at Tokyo, Hedo, and Ny-Ålesund, thus confirming the clear and consistent relationship between $M_{BC}$ (COSMOS) and $M_{BC}$ (SP2). Miyakawa et al. (2017) also reported a strong correlation ($r^2$ = 0.92; slope 1.14) of $M_{BC}$ (COSMOS) with $M_{BC}$ (SP2) at Fukue in spring 2015 by using an SP2 maintained and calibrated by the Japan Agency for Marine-Earth Science and Technology.

#### 3.1.2 Alert

Long-term measurements of BC using different manufacturer's model versions of SP2s have been conducted at Alert since 2011 (Sharma et al., 2017). In this study, we used the data obtained by EC-SP2 (manufacturer's model version of "SP2-D" with eight channels; see Sect. 2.1) from January to May 2018 for comparison with the COSMOS data. The EC-SP2 and COSMOS aspired sample air from a common inlet with a $PM_1$ size cut. Fig. 4a shows the number and mass size distributions of BC averaged over the observation period. The mode diameter of the average mass size distribution of BC was ~210 nm, which is similar to those observed previously at Alert (Sharma et al., 2017) and those observed by an aircraft measurements over Alert (Schulz et al., 2019). Because the upper limit of the detectable diameter range of BC was ~600 nm for the EC-SP2, we have estimated $M_{BC}$ (SP2) over the range up to 1000 nm by fitting lognormal functions to the measured mass size distributions. The time series of hourly values of $M_{BC}$ (COSMOS) and $M_{BC}$ (SP2) (Fig. 4b) were strongly correlated ($r^2$ = 0.92) and the slope of the correlation was 1.02 (Fig. 4c). These results show that the agreement between $M_{BC}$

https://doi.org/10.5194/acp-2020-1190
Preprint. Discussion started: 11 December 2020



(COSMOS) and $M_{BC}$ (SP2) was within 10% at Alert, on average. Although this agreement was consistent with those reported in previous studies using UT-SP2 (Kondo et al., 2011, Ohata et. al., 2019), it should be noted that there were some differences between $M_{BC}$ (SP2) measured by the EC-SP2 and that by the UT-SP2. The EC-SP2 was calibrated by Aquadag samples at Alert during the observation period and also calibrated by fullerene soot samples at Paul Scherrer Institute (PSI) in Switzerland after the observation period. Because the sensitivity of the incandescence signals of the SP2 to Aquadag is higher than that to fullerene soot, the calibration curve for Aquadag needs correction to obtain the fullerene-soot equivalent calibration curve (Baumgardner et al., 2012). Also, to make this correction, assumptions of the effective density ($\rho_{eff}$) values of Aquadaq (Moteki and Kondo, 2010; Gysel et al., 2011), which depend on mobility diameter of Aquadag, are needed since a differential mobility analyzer (DMA) is used for the on-site calibration at Alert instead of an aerosol particle mass analyzer (APM) or a centrifugal particle mass analyzer. The $\rho_{eff}$ values of Aquadag samples can depend on their batches (Gysel et al., 2011). In the previous study by Sharma et al. (2017), the constant value of $\rho_{eff}$ (= 0.7 g cm$^{-3}$) for Aquadag was assumed to derive $M_{BC}$ (SP2) at Alert.

However, we have found that $M_{BC}$ (SP2) at Alert highly depended on the assumed $\rho_{eff}$ values of Aquadag used for the on-site calibration with a DMA. Because of this, we used the calibration curve obtained by fullerene soot with an APM at PSI after the observation period for this study. The conditions of the EC-SP2 might be slightly different between during and after the observation period, which may lead to additional uncertainties for $M_{BC}$ (SP2) at Alert. In addition, the upper limit of the detectable diameter of BC for the EC-SP2 ($D_m$ ~600 nm) was lower than that for the UT-SP2 ($D_m$ ~850 nm), although the above-mentioned extrapolation up to 1000 nm was made to derive $M_{BC}$ (SP2) at Alert. Despite these differences between EC-SP2 and UT-SP2, $M_{BC}$ (COSMOS) and $M_{BC}$ (SP2) agreed to within 10% at Alert, supporting previous studies (Kondo et al., 2011, Ohata et. al., 2019) which reported the stability of the relationship between $M_{BC}$ (COSMOS) and $M_{BC}$ (SP2) at various sites.

### 3.2 COSMOS–MAAP comparison

#### 3.2.1 Fukue

Kanaya et al. (2013, 2016, 2020) made simultaneous measurements of $M_{BC}$ (COSMOS) and $b_{abs}$ (MAAP) at Fukue for about 10 years (April 2009 – May 2019). The air inlet for the MAAP and COSMOS was equipped with a $PM_1$ cyclone after November 2011. Before that a PM2.5 cyclone was used instead. Correlations of $b_{abs}$ (MAAP) with $M_{BC}$ (COSMOS) were strong ($r^2$ = 0.94) and MAC (MAAP) for the entire period was found to be 10.8 m$^2$ g$^{-1}$ (Fig. 5). Because the correlation of $b_{abs}$ (MAAP) with $M_{BC}$ (COSMOS) was also strong for individual years (Fig. 6), MAC (MAAP) for each year was also derived (Fig. 7a and Table 1). $M_{BC}$ (COSMOS) decreased by about 50% during this period, owing to a large decrease of BC emissions in China (Kanaya et al., 2020). However, the yearly

https://doi.org/10.5194/acp-2020-1190
Preprint. Discussion started: 11 December 2020


Atmospheric Chemistry and Physics Discussions

average MAC (MAAP) was stable at 11.1 ± 1.1 (1σ) m$^2$ g$^{-1}$, despite the large change in $M_{BC}$ (COSMOS).

#### 3.2.2 Pallastunturi

In the Arctic, $b_{abs}$ (MAAP) measurements have been made since 2007 at the Global Atmospheric Watch (GAW) station at Pallastunturi (Pallas, hereafter) (68.0°N, 24.0°E, 565 m above sea level) by the Finnish Meteorological Institute (Hyvärinen et al., 2011). $PM_{10}$ and $PM_1$ inlets were used for MAAP and COSMOS, respectively. $M_{BC}$ (COSMOS) measurements began in July 2019; we used the data collected up to July 2020 in this study. The $M_{BC}$ (COSMOS) data for about 3 months (February to April 2020) were unusable due to an air sampling problem.

The 1-h and 24-h values of $M_{BC}$ (COSMOS) and $b_{abs}$ (MAAP) (Fig. 8a and 8b) were strongly correlated with $r^2$ = 0.93 and $r^2$ = 0.95, respectively (Fig. 8c and 8d). From the slope of the correlation, MAC (MAAP) was determined to be 13.0 m$^2$ g$^{-1}$.

The average of the overall MAC (MAAP) values for Pallas and Fukue was 12.1 ± 1.3 (1σ; 11% of the average) m$^2$ g$^{-1}$ (Table 2), with the difference between the two sites being about 17%; this is somewhat greater than the variability of MAC (MAAP) at Fukue and the uncertainty of $M_{BC}$ (COSMOS). This difference may reflect in part the greater effect on $b_{abs}$ (MAAP) at Pallas of dust particles passing through the $PM_{10}$ inlet (discussed in Sect. 2). This average MAC value suggests that the manufacturer's recommended value of MAC (MAAP) of 6.6 m$^2$ g$^{-1}$ is too low by a factor of about two. One possible reason for this underestimate is the corresponding overestimates of $M_{BC}$ (GRM) in Eq. (6) and underscores the importance of the absolute accuracy of $M_{BC}$ measurements used to determine MAC. Another reason could be that the difference in microphysical properties of BC (e.g. coating thickness) and properties of co-existing LSPs lead to the different MAC (MAAP) values. Because these are the only available MAC (MAAP) data sets derived using $M_{BC}$ (COSMOS), further study is required to evaluate the spatial variability of MAC (MAAP).

### 3.3 COSMOS–PSAP/CLAP comparison

#### 3.3.1 Barrow

Simultaneous measurements of $PM_1$ for $M_{BC}$ (COSMOS) and $b_{abs}$ (PSAP/CLAP) began at Barrow in 2012 (Sinha et al., 2017). At Barrow, both the PSAP and CLAP aspired ambient air using $PM_1$ and $PM_{10}$ impactors alternately for 30 min of each hour. Here we used the data from the PSAP/CLAP equipped with $PM_1$ impactor. In this study, we used the data from the PSAP in 2012–2015 and the data from CLAP in 2016–2019 (Fig. 9). Because the 24-h averaged $b_{abs}$ (PSAP) and $b_{abs}$ (CLAP) values agreed to within 2% during 2012–2015 (Sinha et al., 2017) when the PSAP and CLAP overlapped, we consider the two instruments to be equivalent. The $M_{BC}$ (COSMOS) data from June 2018 to May 2019

https://doi.org/10.5194/acp-2020-1190
Preprint. Discussion started: 11 December 2020




were unusable due to problems with the COSMOS instrument. The $b_{abs}$ (PSAP/CLAP) and $M_{BC}$ (COSMOS) were strongly correlated ($r^2$ = 0.88; Fig. 9c) and the MAC (PSAP/CLAP) derived from 1-h averaged data for the whole period was 10.8 $m^2$ $g^{-1}$ (Table 3). Average MAC during 2012–2018 was stable at 11.0 ± 1.1 (1σ) $m^2$ $g^{-1}$ (Fig. 7b and Table 3). Yearly $M_{BC}$ (COSMOS) values did not exhibit large changes during this period. The correlation between $b_{abs}$ (CLAP) and $M_{BC}$ (COSMOS) during June–December 2019 was weak (Table 3), indicating that either CLAP or COSMOS results might not have been accurate during this period. Therefore, in Table 3 we calculated the average MAC (PSAP/CLAP) by omitting the MAC value for 2019.

### 3.3.2 Ny-Ålesund

Simultaneous measurements of $M_{BC}$ (COSMOS) for $PM_1$ and $b_{abs}$ (PSAP) for $PM_{10}$ began at Ny-Ålesund in 2012 (Sinha et al., 2017; Fig. 10). The 1-h and 24-h averaged $b_{abs}$ (PSAP) at λ = 550 nm and $M_{BC}$ (COSMOS) were well correlated ($r^2$ = 0.76–0.82) and the average MAC (PSAP) for the whole period was 14.4–15.2 $m^2$ $g^{-1}$ (Fig. 7c and Table 4). The correlation between $b_{abs}$ (PSAP) and $M_{BC}$ (COSMOS) during April–December 2012 was weak for unknown reasons. Except for this period, average MAC (PSAP) during 2013–2016 was 15.2 ± 2.5 (1σ) $m^2$ $g^{-1}$. These values are larger than those at Barrow (Table 6), possibly because of the greater effect on $b_{abs}$ (PSAP) of dust particles measured with a $PM_{10}$ size cut.

### 3.3.3 Alert

Measurements of $M_{BC}$ (COSMOS) at Alert began in January 2018. A $PM_1$ cyclone was used for the COSMOS and a $PM_1$ impactor for the PSAP and two CLAP instruments (CLAP1, CLAP2). The time series of 1-h and 24-h averaged $M_{BC}$ (COSMOS) and $b_{abs}$ (PSAP; λ = 550 nm) for 2018–2019 were strongly correlated ($r^2$ ~0.96; Fig. 11). The values of average MAC (PSAP; λ= 550 nm) for the whole period were 13.9 $m^2$ $g^{-1}$ and 14.0 $m^2$ $g^{-1}$ for the 1-h and 24-h averaged data, respectively. The results of the same analyses for other wavelengths of the PSAP and the two CLAPs show that the strength of the correlation depended little on wavelength (Table 5). The $b_{abs}$, and therefore the MAC, for the PSAP and the two CLAP instruments (CLAP1, CLAP2) agreed to within 8%, indicating little difference in the performance of these instruments. Year-to-year variations of MAC (PSAP; λ= 550 nm) are also shown in Table 6. Average MAC (PSAP) during 2018–2019 was 13.9 $m^2$ $g^{-1}$ for the 1-h data.

The correlation of $b_{abs}$ (PSAP) with $M_{BC}$ (COSMOS) was somewhat stronger at Alert than at Barrow (Table 7), and MAC (PSAP) at Alert was about 21% higher than at Barrow. Alert is more distant from continental sources of aerosols than Barrow (Fig. 1). The stronger correlation of $b_{abs}$ (PSAP) with $M_{BC}$ (COSMOS) at Alert suggests that environmental conditions including LSP/BC ratios and mixing states of BC were more stable at Alert. We found that at Alert $b_{abs}$ (PSAP) data with loading and scattering corrections were strongly correlated with the uncorrected $b_{abs}$ (PSAP) data and the contribution of the

https://doi.org/10.5194/acp-2020-1190
Preprint. Discussion started: 11 December 2020

Atmospheric Chemistry and Physics Discussions

loading and scattering corrections was about 35%, on average. In contrast, the contribution of these corrections was about 63% at Barrow. This indicates that LSP/BC ratio was small and stable at Alert, showing small influences of LSPs on derived $b_{abs}$ (PSAP) at Alert. The enhancement in absorption due to scattering by particles (i.e., the second term of Eq. (14) in Bond et al. (1999)) was about 18% of the uncorrected $b_{abs}$ (i.e., the first term of the same equation) at Alert, on average. However, this feature might be specific to Alert and may be different at other sites. Thus, the precision of $b_{abs}$ extracted from PSAP/CLAP depends on location, especially distance from major sources of aerosols. Further analyses considering the effects of LSP/BC ratios may give further insight.

### 3.4 COSMOS–Aethalometer comparison at Alert

At Alert in 2018, $b_{abs}$ was measured by an Aethalometer at wavelengths of 370, 470, 520, 590, 660, 880, and 950 nm without any particle size cut (Table 8). Overall, the correlations of $b_{abs}$ (Aethalometer; $\lambda$ = 590 nm) with $M_{BC}$ (COSMOS) at Alert (Fig. 12) were somewhat lower ($r^2$ = 0.90 for 1-h data) than those of $b_{abs}$ (PSAP) with $M_{BC}$ (COSMOS) (Fig. 11), but the correlations of the both 1-h and 24-h averaged $b_{abs}$ (Aethalometer) were sufficiently high to estimate $M_{BC}$ with reasonable accuracy at Alert. The MAC (PSAP) agreed with MAC (Aethalometer) within about 10% at three wavelengths (Table 9). This agreement is consistent with the results by Backman et al. (2017), who showed that the correction factor $C_f$ of 3.45 for Aethalometer harmonizes $b_{abs}$ (Aethalometer) with $b_{abs}$ (PSAP), $b_{abs}$ (CLAP), and $b_{abs}$ (MAAP) at Arctic sites.

### 3.5 Variability of MAC and $r^2$

In previous sections, we showed that the MAC values depended on observation site. The MAC ($\lambda$ = 550 nm) and $r^2$ values determined in this study were summarized in Table 10. Here, the MAC (MAAP; $\lambda$ ~637 nm) and MAC (Aethalometer; $\lambda$ = 520 nm) values were adjusted to those at $\lambda$ = 550 nm by assuming an absorption Ångstrom exponent of 1.0 (i.e., a $\lambda^{-1}$ relationship). The unit-to-unit variations of $b_{abs}$ measurements were reported to be within 5% for MAAP (Müller et al., 2011), 6% for PSAP (Bond et al.,1999), and 4% for CLAP (Ogren et al., 2017), if the careful calibration of flows and filter sampling spot sizes of these instruments are made for individual units. Therefore, the spatial variations of MAC values observed in this study likely reflects the difference of aerosol properties at the observation sites.

The values of MAC (MAAP) determined at Fukue and Pallas differ by about 17%. Part of this difference may reflect the difference in the inlet size cut, as mentioned in Sect. 3.2.2. Because these are the only available MAC (MAAP) data sets derived from $M_{BC}$ (COSMOS), it is difficult to evaluate spatial variability further.

The values of MAC (PSAP) at Alert and MAC (PSAP/CLAP) at Barrow were both determined with

https://doi.org/10.5194/acp-2020-1190
Preprint. Discussion started: 11 December 2020



$PM_1$ size cut and they differed by about 21%. This difference may partly reflect a difference in the precision of $b_{abs}$ measurements at the two sites. In fact, the correlations of $b_{abs}$ (PSAP) with $M_{BC}$ (COSMOS) at Alert were somewhat higher ($r^2$ = 0.96–0.97) than those of $b_{abs}$ (PSAP/CLAP) at Barrow ($r^2$ = 0.84–0.87). In addition, differences in aerosol properties including mixing states of BC at these sites could contribute to the different MAC values, although that cannot be assessed with this dataset. At Ny-Ålesund, where a $PM_{10}$ inlet was used, the MAC values were higher than those at Barrow and Alert. Also, the $r^2$ values at Ny-Ålesund ($r^2$ = 0.84–0.89) were lower than those at Alert. Effects of particles larger than 1 μm including dust may partly contribute to the larger MAC and lower $r^2$ values at Ny-Ålesund.

We have shown that $b_{abs}$ values obtained by MAAP, PSAP, CLAP, and Aethalometer were in general strongly correlated with $M_{BC}$ (COSMOS) at all four Arctic sites, although the strength of the correlation differed somewhat among the sites. The average values of MAC (λ = 550 nm) for these sites were 13.8 ± 2.0 (1$\sigma$; 15% of the average) and 14.1 ± 2.5 (1σ; 18%) $m^2\ g^{-1}$ for 1-h and 24-h data, respectively (Table 9). However, these correlations may not hold outside the Arctic, where environmental conditions, especially the amount of interference by LSPs, can be very different.

Zanatta et al. (2016) reported the average MAC value at λ = 637 nm for nine European back ground sites to be 10.0 $m^2\ g^{-1}$, using elemental carbon mass concentrations measured by the thermal-optical transmittance method with the EUSAAR-2 protocol, instead of $M_{BC}$ (COSMOS). From this MAC (λ = 637 nm) value, the value of MAC at λ = 550 nm is calculated to be 11.6 $m^2\ g^{-1}$ by assuming an absorption Ångstrom exponent of 1.0. Although their MAC values were generally obtained using $PM_{10}$ inlets or without particle size-cuts, their average MAC value (= 11.6 $m^2\ g^{-1}$) is by about 16% lower than our average MAC value (about 14.0 $m^2\ g^{-1}$) determined in this study. This discrepancy may partly due to the difference of the methods to determine absolute mass concentrations of BC.

Mason et al. (2018) derived the values of MAC (PSAP) and MAC (CLAP) for $PM_1$ size range in biomass burning and agriculture fire plumes during the $SEAC^4RS$ aircraft observation campaign by using $M_{BC}$ (SP2) data. They reported the MAC (PSAP; λ = 550 nm) and MAC (CLAP; λ = 550 nm) values to be 21.0 and 26.5 $m^2\ g^{-1}$, respectively, which are by about 50% larger than the average MAC value (about 14.0 $m^2\ g^{-1}$) determined in this study. Although the reason for their very high MAC values were not clear, one possible explanation given by Mason et al. (2018) is that the considerable amount of additional absorber other than BC, including tar balls, might exist in their samples. Also, strong lens effects by the BC coatings could contribute to the high MAC values. Thus, the MAC values can be highly dependent on environmental conditions and those reported in the present study are considered to be site-specific values, although the variability (1$\sigma$) of our MAC values in the 4 Arctic sites was within 18% of the average MAC value (about 14.0 $m^2\ g^{-1}$).

https://doi.org/10.5194/acp-2020-1190
Preprint. Discussion started: 11 December 2020




**4 Summary and conclusions**

Long-term measurements of $M_{BC}$ by ground-based instruments are warranted for investigating changes in the emission, transport, and deposition of BC. Various types of filter-based absorption photometers, including multi-angle absorption photometer (MAAP), particle absorption soot photometer (PSAP), continuous light absorption photometer (CLAP), and Aethalometer, have been used in the Arctic. To date, the accuracy of $M_{BC}$ estimated from absorption coefficients ($b_{abs}$) measured by these instruments have not been adequately assessed, mainly because of a lack of simultaneous and reliable $M_{BC}$ measurements.

In this paper, we introduce a systematic methodology to derive $M_{BC}$ from $b_{abs}$ measured by these instruments. To obtain accurate values of $M_{BC}$, we used a filter-based absorption photometer with a heated inlet (COSMOS), which we calibrated to within 10% uncertainty with an SP2 deployed in Tokyo. Individual COSMOS instruments used for field observations were calibrated against the standard COSMOS to within about 10%. The accuracy of $M_{BC}$ (COSMOS) has previously been demonstrated to be about 15% by comparison with $M_{BC}$ (SP2) in Asia and the Arctic. The effect on $M_{BC}$ (COSMOS) of interference by light-absorbing $FeO_x$ particles was estimated to be only a few percent, owing partly to the particle-size cut off of 1 μm by the $PM_1$ cyclone used. This effect may be somewhat higher for the other filter-based absorption photometers equipped with $PM_{10}$ particle-size cut. The two necessary conditions for application of our method are a high correlation of $b_{abs}$ with independently measured $M_{BC}$ and long-term stability of the slope of the correlation, which represents the MAC.

We compared $b_{abs}$ (MAAP) and $M_{BC}$ (COSMOS) determined at Fukue for about 10 years and at Pallas for about 1 year. $b_{abs}$ (MAAP) was highly correlated with $M_{BC}$ (COSMOS) at these sites. MAC (MAAP) at Fukue was stable at 11.1 ± 1.1 $m^2$ $g^{-1}$, despite a 50% decrease in $M_{BC}$ (COSMOS) during this period. The average MAC (MAAP) at these sites was 12.1 ± 1.3 $m^2$ $g^{-1}$. The MAC (MAAP) recommended by the manufacturer is about half the present value, indicating a similar overestimation of $M_{BC}$ (MAAP).

We also compared $b_{abs}$ (PSAP/CLAP) with $M_{BC}$ (COSMOS) at Barrow ($PM_1$) for 7 years, Ny-Ålesund ($PM_{10}$) for 4 years, and Alert ($PM_1$) for 2 years. $b_{abs}$ (PSAP/CLAP) was highly correlated with $M_{BC}$ (COSMOS) at these sites. The MAC (PSAP/CLAP) at $\lambda$ = 550 nm was 11.0 ± 1.0 $m^2$ $g^{-1}$ at Barrow. The values of MAC (PSAP) at $\lambda$ = 550 nm for Ny-Ålesund and Alert were 15.2 ± 2.5 $m^2$ $g^{-1}$ and 13.9 ± 0.6 $m^2$ $g^{-1}$, respectively.

At Alert, correlations of 24-h averaged $b_{abs}$ (Aethalometer) with $M_{BC}$ (COSMOS) were also high ($r^2$ = 0.86–0.93), but varied with wavelength. MAC (Aethalometer; $\lambda$ = 520 nm) without any particle size cut was about 14.1 $m^2$ $g^{-1}$.

Our results show that $M_{BC}$ can be derived from $b_{abs}$ obtained from MAAP, PSAP, CLAP, and

https://doi.org/10.5194/acp-2020-1190
Preprint. Discussion started: 11 December 2020


Atmospheric Chemistry and Physics Discussions

Aethalometer measurements with reasonable accuracy by using MAC obtained from the slope of the $b_{abs}$–$M_{BC}$ correlation, especially for long data-averaging times. However, scatter in $b_{abs}$–$M_{BC}$ (COSMOS) correlations indicate that the accuracy of this method will be somewhat lower than that achieved by direct measurement of $M_{BC}$ (COSMOS). We also caution that the reliability of the use of $b_{abs}$ data to derive $M_{BC}$ at other locations, especially those outside the Arctic, is unknown. Rigorous comparisons with COSMOS data, such as those of this study, are required if use of our method is to expand beyond the Arctic region. Moreover, the key parameter in converting $b_{abs}$ measured by filter-based absorption photometer to $M_{BC}$ is MAC, for which accurate determination can be achieved only by long-term comparisons with a COSMOS or SP2. Short-term comparisons will be of limited value for understanding the variability of MAC.

**Data availability**

The observational data set used in this publication is available online (https://ads.nipr.ac.jp/dataset/A20201120-001).

**Author contributions**

SO, TM, and YKo designed the study, conducted the analyses, and wrote the paper. SS and DV contributed to the field observations and data analysis of SP2, PSAP, CLAP, and Aethalometer at Alert. AH, EAs, JB, and HS contributed to the field observations and data analysis of MAAP at Pallas. EAn contributed to the field observations and data analysis of PSAP and CLAP at Barrow. PT obtained and analysed PSAP data at Ny-Ålesund. YKa contributed to the field observations and data analysis of MAAP and COSMOS at Fukue. AY and NM obtained and analysed SP2 data at Fukue. SO, TM, YKo, MK, YZ, JM, and NO contributed to instrument maintenance and data analysis of COSMOS.

**Competing interests**

The authors declare that they have no conflicts of interest.

**Acknowledgements**

We thank Kevin Rawlings and Melody Fraser of Environment and Climate Change (Canada) and CFS Alert for operations and maintenance of the Alert site. We thank Bryan Thomas, Peter Detwiler, and Ross Peterson for supporting the measurements at Barrow. This research was performed by the Environment Research and Technology Development Fund (JPMEERF20142003, JPMEERF20172003, JPMEERF20202003, and JPMEERF20205001) of the Environmental Restoration and Conservation Agency of Japan; the Japanese Ministry of Education, Culture, Sports, Science, and Technology; the

Japan Society for the Promotion of Science KAKENHI Grants (JP12J06736, JP1604452, JP23221001, JP26241003, JP26701004, JP16H01770, JP17H04709, JP18H03363, JP19K20441, and JP20H00638); the Arctic Challenge for Sustainability (ArCS) project (JPMXD1300000000); the Arctic Challenge for Sustainability II (ArCS II) project (JPMXD1420318865); and a grant for the Global Environmental Research Coordination System from the Ministry of the Environment, Japan. Pallas measurements were conducted under the financial support of the ACTRIS by the European Union's Horizon 2020 research and innovation programme under grant agreement no. 654109. The research was also supported by Academy of Finland via project NABCEA (grant no. 29664) and the 16ENV02 Black Carbon project of the European Union through the European Metrology Programme for Innovation and Research (EMPIR).

**References**

Arctic Monitoring and Assessment Programme (AMAP): AMAP Assessment 2015: Black carbon and ozone as Arctic climate forcers, Oslo, Norway, pp. vii + 116, 2015.

Baumgardner, D., Popovicheva, O., Allan, J., Bernardoni, V., Cao, J., Cavalli, F., Cozic, J., Diapouli, E., Eleftheriadis, K., Genberg, P. J., Gonzalez, C., Gysel, M., John, A., Kirchstetter, T. W., Kuhlbusch, T. A. J., Laborde, M., Lack, D., Müller, T., Niessner, R., Petzold, A., Piazzalunga, A., Putaud, J. P., Schwarz, J., Sheridan, P., Subramanian, R., Swietlicki, E., Valli, G., Vecchi, R., and Viana, M.: Soot reference materials for instrument calibration and intercomparisons: A workshop summary with recommendations, Atmos. Meas. Tech., 5, 1869–1887, https://doi.org/10.5194/amt-5-1869-2012, 2012.

Backman, J., Schmeisser, L., Virkkula, A., Ogren, J. A., Asmi, E., Starkweather, S., Sharma, S., Eleftheriadis, K., Uttal, T., Jefferson, A., Bergin, M., Makshtas, A., Tunved, P., and Fiebig, M.: On Aethalometer measurement uncertainties and an instrument correction factor for the Arctic, Atmos. Meas. Tech., 10, 5039–5062, https://doi.org/10.5194/amt-10-5039-2017, 2017.

Bergstrom, R. W.: Predictions of the spectral absorption and extinction coefficients of an urban air pollution aerosol model, Atmos. Environ., 6, 247–258, https://doi.org/10.1016/0004-6981(72)90083-2, 1972.

Bond, T. C., Anderson, T. L., and Campbell, D.: Calibration and Intercomparison of Filter-Based Measurements of Visible Light Absorption by Aerosols, Aerosol Sci. Tech., 30, 6, 582–600, https://doi.org/10.1080/027868299304435, 1999.

Bond, T. C., Habib, G., and Bergstrom, R. W.: Limitations in the enhancement of visible light absorption due to mixing state, J. Geophys. Res. Atmos., 111, D20211, https://doi.org/10.1029/2006JD007315., 2006.

Bond, T. C., Doherty, S. J., Fahey, D. W., Forster, P. M., Berntsen, T., Deangelo, B. J., Flanner, M. G., Ghan, S., Kärcher, B., Koch, D., Kinne, S., Kondo, Y., Quinn, P. K., Sarofim, M. C., Schultz, M. G., Schulz, M., Venkataraman, C., Zhang, H., Zhang, S., Bellouin, N., Guttikunda, S. K., Hopke, P. K., Jacobson, M. Z., Kaiser, J. W., Klimont, Z., Lohmann, U., Schwarz, J. P., Shindell, D., Storelvmo, T., Warren, S. G., and Zender, C. S.: Bounding the role of black carbon in the climate system: A scientific assessment, J. Geophys. Res. Atmos., 118, 1–173, https://doi.org/10.1002/jgrd.50171, 2013.

Eyring, V., Bony, S., Meehl, G. A., Senior, C. A., Stevens, B., Stouffer, R. J., and Taylor, K. E.: Overview of the Coupled Model Intercomparison Project Phase 6 (CMIP6) experimental design and organization, Geosci. Model Dev., 9, 1937–1958, https://doi.org/10.5194/gmd-9-1937-2016, 2016.

Flanner, M. G., Zender, C. S., Hess, P. G., Mahowald, N. M., Painter, T. H., Ramanathan, V., and Rasch, P. J.: Springtime warming and reduced snow cover from carbonaceous particles, Atmos. Chem. Phys., 9, 2481–2497, https://doi.org/10.5194/acp-9-2481-2009, 2009.

Gysel, M., Laborde, M., Olfert, J. S., Subramanian, R., and Gréhn, A. J.: Effective density of Aquadag and fullerene soot black carbon reference materials used for SP2 calibration, Atmos. Meas. Tech., 4, 2851–2858, https://doi.org/10.5194/amt-4-2851-2011, 2011.

Hansen, A. D. A., Rosen, H., and Novakov, T.: The aethalometer – an instrument for the real-time measurement of optical absorption by aerosol particles, Sci. Total Environ., 36, 191–196, 1984.

Huffman, D. R. and Stapp, J. L.: Interstellar dust and related topics, edited by: Greenberg, J. M. and Van de Hulst, H. C., Reidel, Boston, pp. 297–301, 1973.

Hyvärinen, A. P., Kolmonen, P., Kerminen, V. M., Virkkula, A., Leskinen, A., Komppula, M., Hatakka, J., Burkhart, J., Stohl, A., Aalto, P., Kulmala, M., Lehtinen, K. E. J., Viisanen, Y., and Lihavainen, H.: Aerosol black carbon at five background measurement sites over Finland, a gateway to the Arctic, Atmos. Environ., 45, 4042–4050, https://doi.org/10.1016/j.atmosenv.2011.04.026, 2011.

Irwin, M., Kondo, Y., and Moteki, N.: An empirical correction factor for filter-based photo-absorption black carbon measurements, J. Aerosol Sci., 80, 86–97, https://doi.org/10.1016/j.jaerosci.2014.11.001, 2015.

Kanaya, Y., Taketani, F., Komazaki, Y., Liu, X., Kondo, Y., Sahu, L. K., Irie, H., and Takashima, H.: Comparison of black carbon mass concentrations observed by multi-angle absorption photometer (MAAP) and continuous soot-monitoring system (COSMOS) on Fukue Island and in Tokyo, Japan, Aerosol Sci. Tech., 47, 1, 1–10, https://doi.org/10.1080/02786826.2012.716551, 2013.

https://doi.org/10.5194/acp-2020-1190
Preprint. Discussion started: 11 December 2020




Kanaya, Y., Pan, X., Miyakawa, T., Komazaki, Y., Taketani, F., Uno, I., and Kondo, Y.: Long-term observations of black carbon mass concentrations at Fukue Island, western Japan, during 2009–2015: constraining wet removal rates and emission strengths from East Asia, Atmos. Chem. Phys., 16, 10689–10705, https://doi.org/10.5194/acp-16-10689-2016, 2016.

Kanaya, Y., Yamaji, K., Miyakawa, T., Taketani, F., Zhu, C., Choi, Y., Komazaki, Y., Ikeda, K., Kondo, Y., and Klimont, Z.: Rapid reduction in black carbon emissions from China: Evidence from 2009-2019 observations on Fukue Island, Japan, Atmos. Chem. Phys., 20, 6339–6356, https://doi.org/10.5194/acp-20-6339-2020, 2020.

Kondo, Y.: Effects of Black Carbon on Climate: Advances in Measurement and Modeling, Monogr. Environ. Earth Planets, 3, 1–85, https://doi.org/10.5047/meep.2015.00301.0001, 2015.

Kondo, Y., Sahu, L., Kuwata, M., Miyazaki, Y., Takegawa, N., Moteki, N., Imaru, J., Han, S., Nakayama, T., Oanh, N. T. K., Hu, M., Kim, Y. J., and Kita, K.: Stabilization of the mass absorption cross section of black carbon for filter-based absorption photometry by the use of a heated inlet, Aerosol Sci. Tech., 43, 8, 741–756, https://doi.org/10.1080/02786820902889879, 2009.

Kondo, Y., Sahu, L., Moteki, N., Khan, F., Takegawa, N., Liu, X., Koike, M., and Miyakawa, T.: Consistency and traceability of black carbon measurements made by laser-induced incandescence, thermal-optical transmittance, and filter-based photo-absorption techniques, Aerosol Sci. Tech., 45, 2, 295–312, https://doi.org/10.1080/02786826.2010.533215, 2011.

Laborde, M., Mertes, P., Zieger, P., Dommen, J., Baltensperger, U., and Gysel, M.: Sensitivity of the Single Particle Soot Photometer to different black carbon types, Atmos. Meas. Tech., 5, 1031–1043, https://doi.org/10.5194/amt-5-1031-2012, 2012.

Lack, D. A., Cappa, C. D., Covert, D. S., Baynard, T., Massoli, P., Sierau, B., Bates, T. S., Quinn, P. K., Lovejoy, E. R., and Ravishankara, A. R.: Bias in filter-based aerosol light absorption measurements due to organic aerosol loading: Evidence from ambient measurements. Aerosol. Sci. Tech. 42, 1033–1041, https://doi.org/10.1080/02786820802389277, 2008.

Lamb, K. D.: Classification of iron oxide aerosols by a single particle soot photometer using supervised machine learning, Atmos. Meas. Tech., 12, 3885–3906, https://doi.org/10.5194/amt-12-3885-2019, 2019.

Lihavainen, H., Hyvärinen, A., Asmi, E., Hatakka, J., and Viisanen, Y.: Long-term variability of aerosol optical properties in northern Finland, Boreal Env. Res., 20, 526–541, 2015.

https://doi.org/10.5194/acp-2020-1190
Preprint. Discussion started: 11 December 2020


Atmospheric Chemistry and Physics Discussions

Matsui, H., Mahowald, N. M., Moteki, N., Hamilton, D. S., Ohata, S., Yoshida, A., Koike, M., Scanza, R. A., and Flanner, M. G.: Anthropogenic combustion iron as a complex climate forcer, Nat. Commun., 9, https://doi.org/10.1038/s41467-018-03997-0, 2018.

Mason, B., Wagner, N. L., Adler, G., Andrews, E., Brock, C. A., Gordon, T. D., Lack, D. A., Perring, A. E., Richardson, M. S., Schwarz, J. P., Shook, M. A., Thornhill, K. L., Ziemba, L. D., and Murphy, D. M.: An intercomparison of aerosol absorption measurements conducted during the SEAC$^4$RS campaign, Aerosol Sci. Tech., 52, 1012–1027, https://doi.org/10.1080/02786826.2018.1500012, 2018.

Miyakawa, T., Oshima, N., Taketani, F., Komazaki, Y., Yoshino, A., Takami, A., Kondo, Y., and Kanaya, Y.: Alteration of the size distributions and mixing states of black carbon through transport in the boundary layer in east Asia, Atmos. Chem. Phys., 17, 5851–5864, https://doi.org/10.5194/acp-17-5851-2017, 2017.

Miyazaki, Y., Kondo, Y., Sahu, L. K., Imaru, J., Fukushima, N., and Kano, M.: Performance of a newly designed continuous soot monitoring system (COSMOS), J. Environ. Monitor., 10, 1195–1201, https://doi.org/10.1039/b806957c, 2008.

Moteki, N. and Kondo, Y.: Dependence of laser-induced incandescence on physical properties of black carbon aerosols: Measurements and theoretical interpretation, Aerosol Sci. Technol., 44, 8, 663–675, https://doi.org/10.1080/02786826.2010.484450, 2010.

Moteki, N., Adachi, K., Ohata, S., Yoshida, A., Harigaya, T., Koike, M., and Kondo, Y.: Anthropogenic iron oxide aerosols enhance atmospheric heating, Nat. Commun., 8, https://doi.org/10.1038/ncomms15329, 2017.

Müller, T., Henzing, J. S., De Leeuw, G., Wiedensohler, A., Alastuey, A., Angelov, H., Bizjak, M., Collaud Coen, M., Engström, J. E., Gruening, C., Hillamo, R., Hoffer, A., Imre, K., Ivanow, P., Jennings, G., Sun, J. Y., Kalivitis, N., Karlsson, H., Komppula, M., Laj, P., Li, S. M., Lunder, C., Marinoni, A., Martins Dos Santos, S., Moerman, M., Nowak, A., Ogren, J. A., Petzold, A., Pichon, J. M., Rodriquez, S., Sharma, S., Sheridan, P. J., Teinilä, K., Tuch, T., Viana, M., Virkkula, A., Weingartner, E., Wilhelm, R., and Wang, Y. Q.: Characterization and intercomparison of aerosol absorption photometers: result of two intercomparison workshops, Atmos. Meas. Tech., 4, 245–268, https://doi.org/10.5194/amt-4-245-2011, 2011.

Ogren, J. A.: Comment on “calibration and intercomparison of filter-based measurements of visible light absorption by aerosols,” Aerosol Sci. Tech., 44, 8, 589–591, https://doi.org/10.1080/02786826.2010.482111, 2010.

Ogren, J. A., Wendell, J., Andrews, E., and Sheridan, P. J.: Continuous light absorption photometer for long-term studies, Atmos. Meas. Tech., 10, 4805–4818, https://doi.org/10.5194/amt-10-4805-2017, 2017.

Ohata, S., Yoshida, A., Moteki, N., Adachi, K., Takahashi, Y., Kurisu, M., and Koike, M.: Abundance of Light-Absorbing Anthropogenic Iron Oxide Aerosols in the Urban Atmosphere and Their Emission Sources, J. Geophys. Res. Atmos., 123, 8115–8134, https://doi.org/10.1029/2018JD028363, 2018.

Ohata, S., Kondo, Y., Moteki, N., Mori, T., Yoshida, A., Sinha, P. R., and Koike, M.: Accuracy of black carbon measurements by a filter-based absorption photometer with a heated inlet, Aerosol Sci. Tech., 53, 9, 1079–1091, https://doi.org/10.1080/02786826.2019.1627283, 2019.

Oshima, N., Yukimoto, S., Deushi, M., Koshiro, T., Kawai, H., Tanaka, T. Y., and Yoshida, K.: Global and Arctic Radiative Forcing of Anthropogenic Gases and Aerosols in MRI-ESM2.0, Prog. Earth Planet. Sci., 7, 38, https://doi.org/10.1186/s40645-020-00348-w, 2020.

Petzold, A., Kramer, H., and Schönlinner, M.: Continuous measurement of atmospheric black carbon using a multi-angle absorption photometer, Environ. Sci. Pollut. R. Special issue 4, 78–82, 2002.

Petzold, A. and Schönlinner, M.: Multi-angle absorption photometry – A new method for the measurement of aerosol light absorption and atmospheric black carbon, J. Aerosol Sci., 35, 421–441, https://doi.org/10.1016/j.jaerosci.2003.09.005, 2004.Petzold, A., Schloesser, H., Sheridan, P. J., Arnott, W. P., Ogren, J. A., and Virkkula, A.: Evaluation of multiangle absorption photometry for measuring aerosol light absorption, Aerosol Sci. Tech., 39, 1, 40–51, https://doi.org/10.1080/027868290901945, 2005.

Sand, M., Berntsen, T. K., Von Salzen, K., Flanner, M. G., Langner, J., and Victor, D. G.: Response of Arctic temperature to changes in emissions of short-lived climate forcers, Nat. Clim. Change, 6, 286–289, https://doi.org/10.1038/nclimate2880, 2016.

Schmeisser, L., Andrews, E., Ogren, J. A., Sheridan, P., Jefferson, A., Sharma, S., Kim, J. E., Sherman, J. P., Sorribas, M., Kalapov, I., Arsov, T., Angelov, C., Mayol-Bracero, O. L., Labuschagne, C., Kim, S.-W., Hoffer, A., Lin, N.-H., Chia, H.-P., Bergin, M., Sun, J., Liu, P., and Wu, H.: Classifying aerosol type using in situ surface spectral aerosol optical properties, Atmos. Chem. Phys., 17, 12097–12120, https://doi.org/10.5194/acp-17-12097-2017, 2017.

Schmid, H., Laskus, L., Jürgen Abraham, H., Baltensperger, U., Lavanchy, V., Bizjak, M., Burba, P., Cachier, H., Crow, D., Chow, J., Gnauk, T., Even, A., Ten Brink, H. M., Giesen, K. P., Hitzenberger, R., Hueglin, C., Maenhaut, W., Pio, C., Carvalho, A., Putaud, J. P., Toom-Sauntry, D., and Puxbaum, H.: Results of the "carbon conference" international aerosol carbon round robin

https://doi.org/10.5194/acp-2020-1190
Preprint. Discussion started: 11 December 2020




test stage I, Atmos. Environ., 35, 2111–2121, https:doi.org/10.1016/S1352-2310(00)00493-3, 2001.

Schulz, H., Zanatta, M., Bozem, H., Richard Leaitch, W., Herber, A. B., Burkart, J., Willis, M. D., Kunkel, D., Hoor, P. M., Abbatt, J. P. D., and Gerdes, R.: High Arctic aircraft measurements characterising black carbon vertical variability in spring and summer, Atmos. Chem. Phys., 19, 2361–2384, https://doi.org/10.5194/acp-19-2361-2019, 2019.

Schwarz, J. P., Gao, R. S., Fahey, D. W., Thomson, D. S., Watts, L. A., Wilson, J. C., Reeves, J. M., Darbeheshti, M., Baumgardner, D. G., Kok, G. L., Chung, S. H., Schulz, M., Hendricks, J., Lauer, A., Kärcher, B., Slowik, J. G., Rosenlof, K. H., Thompson, T. L., Langford, A. O., Loewenstein, M., and Aikin, K. C.: Single-particle measurements of midlatitude black carbon and light-scattering aerosols from the boundary layer to the lower stratosphere, J. Geophys. Res. Atmos., 111, D16207, https://doi.org/10.1029/2006JD007076, 2006.

Sharma, S., Lavoué, D., Chachier, H., Barrie, L. A. and Gong, S. L.: Long-term trends of the black carbon concentrations in the Canadian Arctic, J. Geophys. Res., 109, D15203, https://doi.org/10.1029/2003JD004331, 2004.

Sharma, S., Andrews, E., Barrie, L. A., Ogren, J. A., and Lavoué, D.: Variations and sources of the equivalent black carbon in the high Arctic revealed by long-term observations at Alert and Barrow: 1989–2003, J. Geophys. Res., 111, D14028, https://doi.org/10.1029/2005JD006581, 2006.Sharma, S., Leaitch, W. R., Huang, L., Veber, D., Kolonjari, F., Zhang, W., Hanna, S. J., Bertram, A. K., and Ogren, J. A.: An evaluation of three methods for measuring black carbon in Alert, Canada, Atmos. Chem. Phys., 17, 15225–15243, https://doi.org/10.5194/acp-17-15225-2017, 2017.

Sinha, P. R., Kondo, Y., Koike, M., Ogren, J. A., Jefferson, A., Barrett, T. E., Sheesley, R. J., Ohata, S., Moteki, N., Coe, H., Liu, D., Irwin, M., Tunved, P., Quinn, P. K., and Zhao, Y.: Evaluation of ground-based black carbon measurements by filter-based photometers at two Arctic sites. J. Geophys. Res. Atmos. 122, 3544–3572. https://doi.org/10.1002/2016JD025843, 2017.

World Meteorological Organization/Global Atmosphere Watch: WMO/GAW aerosol measurement procedures, guidelines, and recommendations, GAW Report No. 227, 2016.

Yoshida, A., Moteki, N., Ohata, S., Mori, T., Tada, R., Dagsson-Waldhauserová, P., and Kondo, Y.: Detection of light-absorbing iron oxide particles using a modified single-particle soot photometer, Aerosol Sci. Tech., 50, 3, i–iv, https://doi.org/10.1080/02786826.2016.1146402, 2016.

Yoshida, A., Ohata, S., Moteki, N., Adachi, K., Mori, T., Koike, M., and Takami, A.: Abundance and Emission Flux of the Anthropogenic Iron Oxide Aerosols From the East Asian Continental

https://doi.org/10.5194/acp-2020-1190
Preprint. Discussion started: 11 December 2020




Outflow, J. Geophys. Res. Atmos., 123, 11, 194–11, 209, https://doi.org/10.1029/2018JD028665, 2018.

Yoshida, A., Moteki, N., Ohata, S., Mori, T., Koike, M., Kondo, Y., Matsui, H., Oshima, N., Takami, A., and Kita, K.: Abundances and Microphysical Properties of Light-Absorbing Iron Oxide and Black Carbon Aerosols Over East Asia and the Arctic, J. Geophys. Res. Atmos., 125, https://doi.org/10.1029/2019JD032301, 2020.

Zanatta, M., Gysel, M., Bukowiecki, N., Müller, T., Weingartner, E., Areskoug, H., Fiebig, M., Yttri, K. E., Mihalopoulos, N., Kouvarakis, G., Beddows, D., Harrison, R. M., Cavalli, F., Putaud, J. P., Spindler, G., Wiedensohler, A., Alastuey, A., Pandolfi, M., Sellegri, K., Swietlicki, E., Jaffrezo, J. L., Baltensperger, U., and Laj, P.: A European aerosol phenomenology-5: Climatology of black carbon optical properties at 9 regional background sites across Europe, Atmos. Environ., 145, 346–364, https://doi.org/10.1016/j.atmosenv.2016.09.035, 2016.

https://doi.org/10.5194/acp-2020-1190
Preprint. Discussion started: 11 December 2020




**Figures**

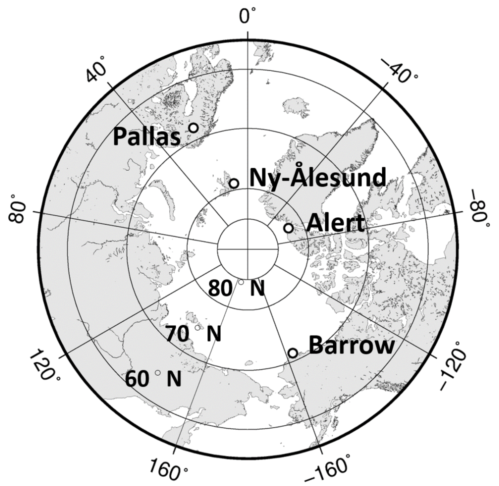


**Fig. 1.** Locations of the sites where BC was measured for this study.

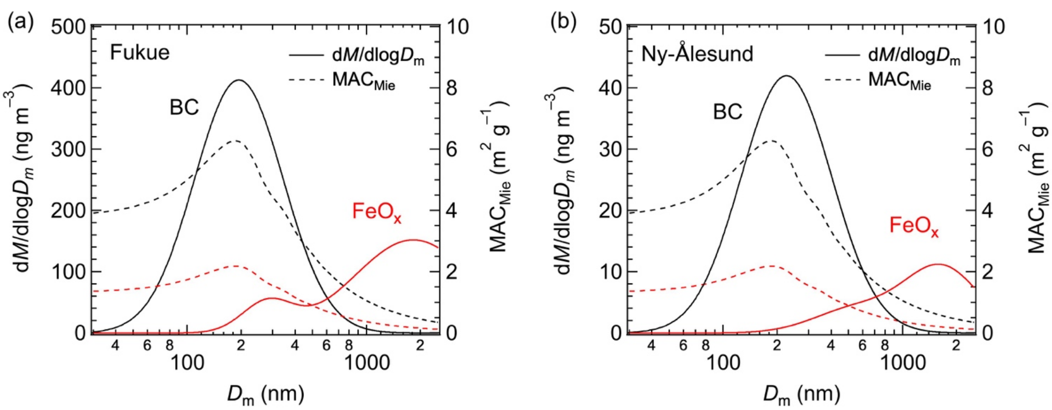


**Fig. 2.** Mass size distributions of BC (black line) and $FeO_x$ (red line) and mass absorption cross sections calculated by Mie theory for BC (black dashed line) and $FeO_x$ (red dashed line) at (a) Fukue in April 2019 and (b) Ny-Ålesund in March 2017. Assumptions for the Mie calculation are given in Sect. 2.

https://doi.org/10.5194/acp-2020-1190
Preprint. Discussion started: 11 December 2020

Atmospheric Chemistry and Physics
Discussions

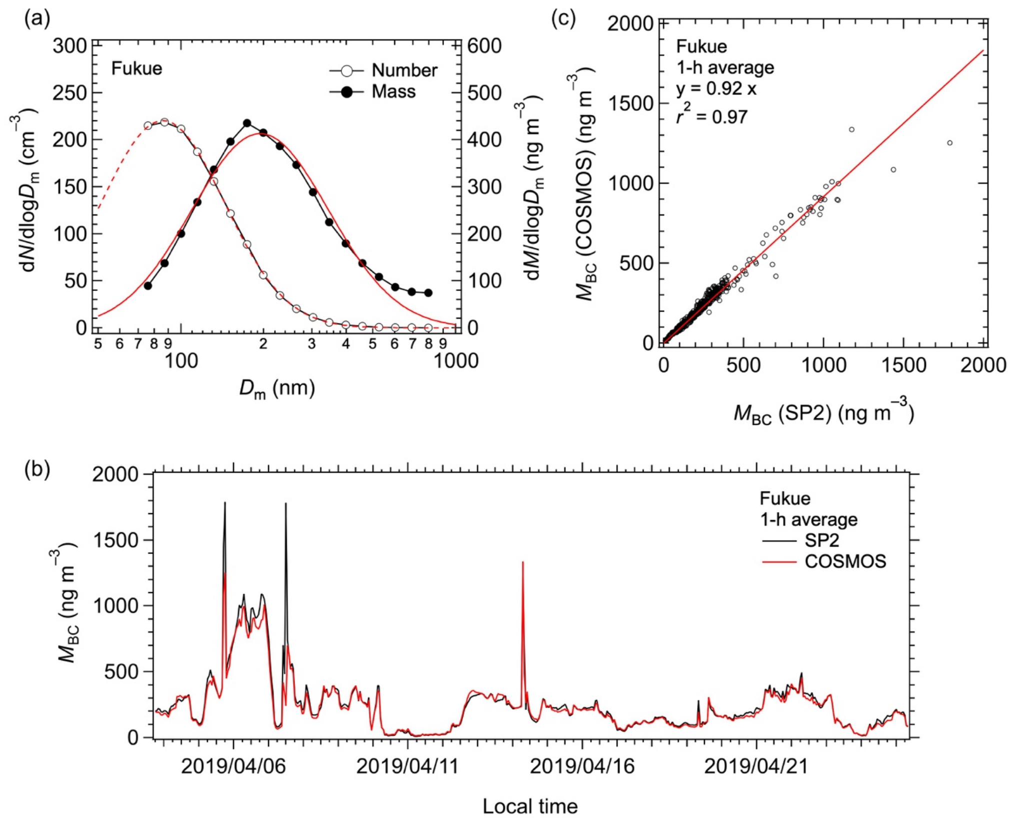


**Fig. 3.** (a) Number and mass size distributions of BC averaged over the observation period at Fukue in April 2019. The dashed (solid) red line is the lognormal fit to the number (mass) size distribution. (b) Time series (1-h data) and (c) correlation of $M_{BC}$ measured by COSMOS and SP2. The solid line in the correlation plot is the least squares fit forced through (0, 0).

https://doi.org/10.5194/acp-2020-1190
Preprint. Discussion started: 11 December 2020




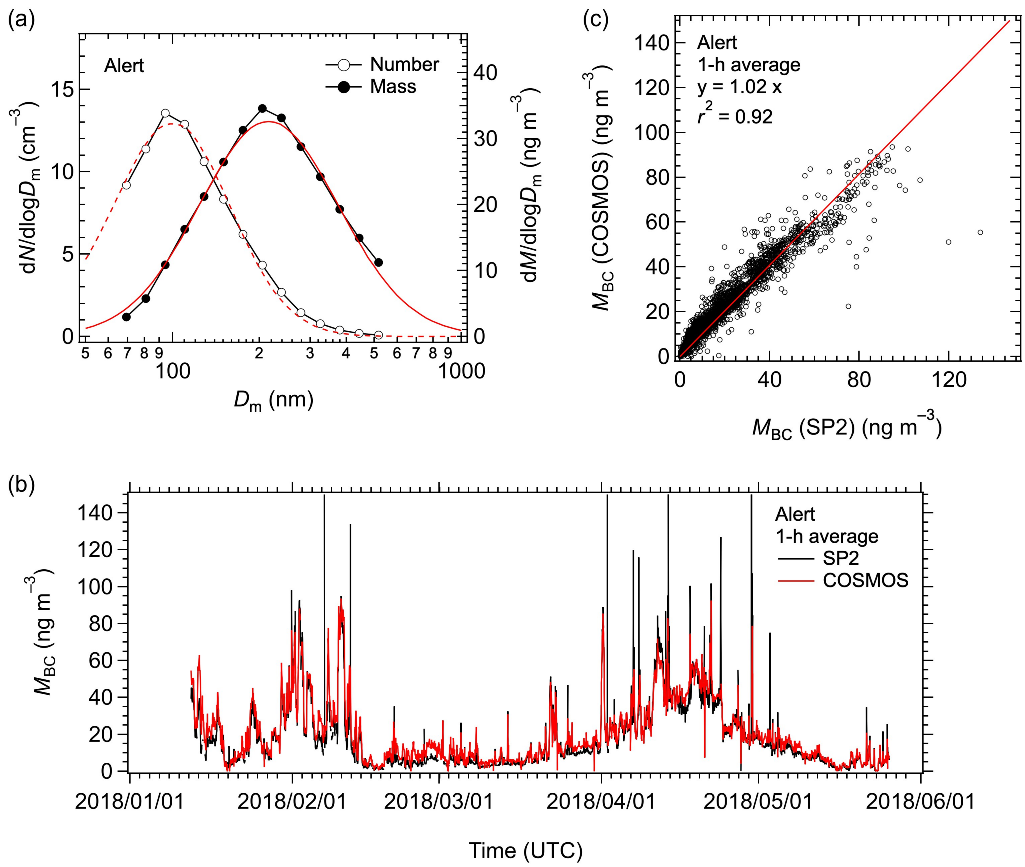


**Fig. 4.** (a) Number and mass size distributions of BC averaged over the observation period at Alert from January to May 2018. The dashed (solid) red line is the lognormal fit to the number (mass) size distribution. (b) Time series (1-h data) and (c) correlation of $M_{BC}$ measured by COSMOS and SP2. The solid line in the correlation plot is the least squares fit forced through (0, 0).

https://doi.org/10.5194/acp-2020-1190
Preprint. Discussion started: 11 December 2020

Atmospheric Chemistry and Physics
Discussions

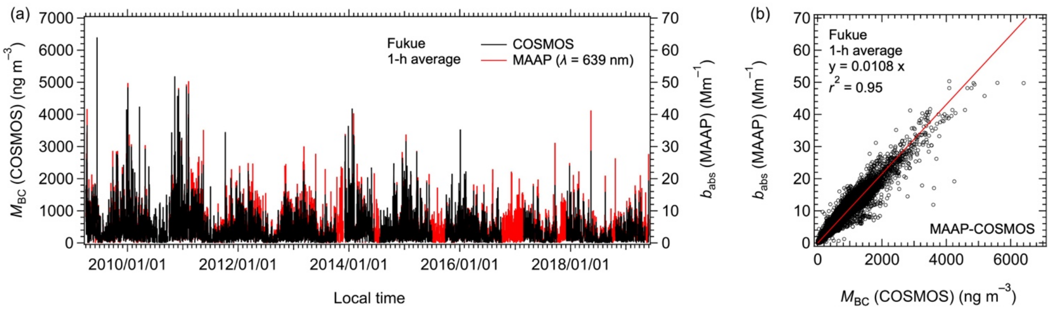


**Fig. 5.** (a) Time series (1-h data) and (b) correlations of $M_{BC}$ (COSMOS) and $b_{abs}$ (MAAP) at Fukue during 2009–2019. The solid line in (b) is the least squares best fit.

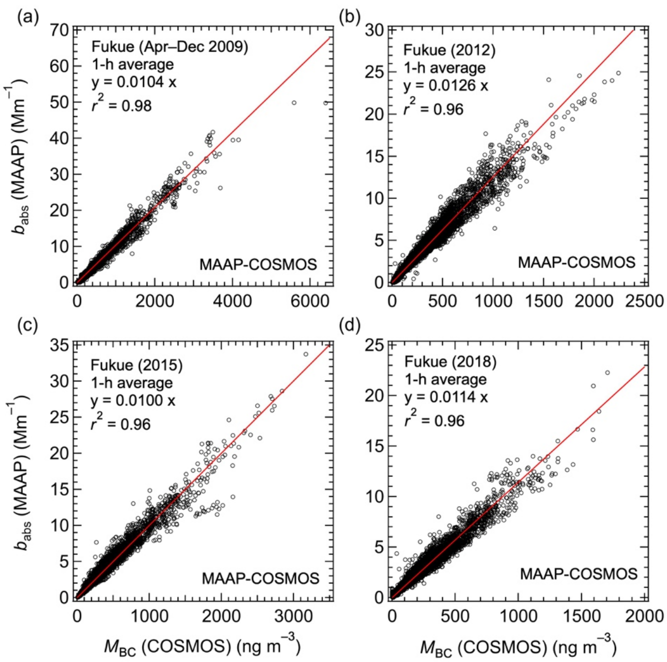


**Fig. 6.** Correlations of 1-h $M_{BC}$ (COSMOS) and $b_{abs}$ (MAAP) at Fukue for (a) 2009, (b) 2012, (c) 2015, and (d) 2018. The data in 2009 were limited during April–December. The solid lines are least squares best fits.

https://doi.org/10.5194/acp-2020-1190
Preprint. Discussion started: 11 December 2020


Atmospheric Chemistry and Physics Discussions
Open Access

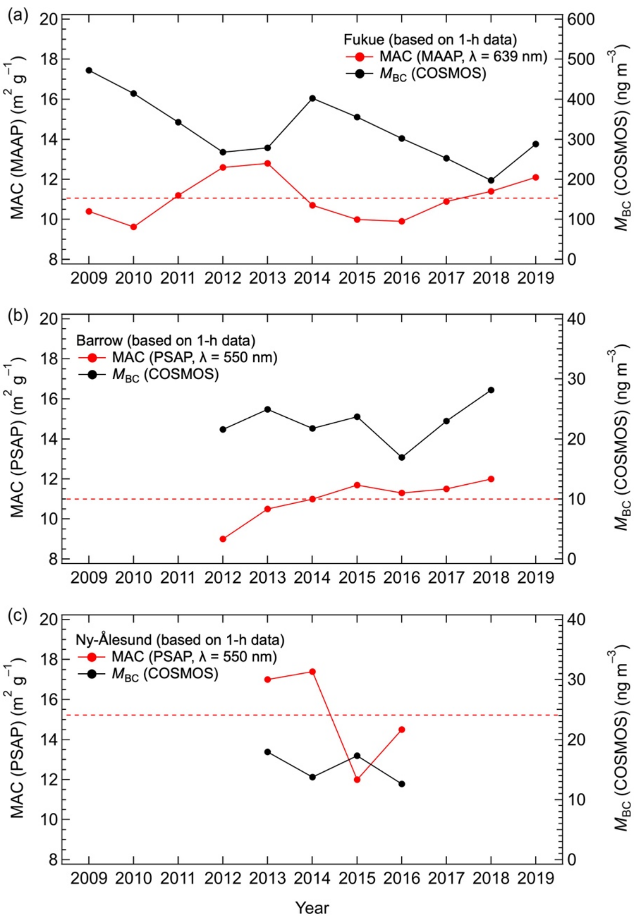


**Fig. 7.** Time series of yearly MAC (MAAP) and $M_{BC}$ (COSMOS) calculated from 1-h data. (a) At
790 Fukue during 2009–2019. The data were limited during April–December 2009 and January–May 2019. (b) At Barrow during 2012–2018. The data were limited during August–December 2012 and January–May 2018. (c) At Ny-Ålesund during 2013–2016. The data were limited during January–September 2016. In each panel, the dashed line shows the average of yearly MAC (MAAP).

https://doi.org/10.5194/acp-2020-1190
Preprint. Discussion started: 11 December 2020


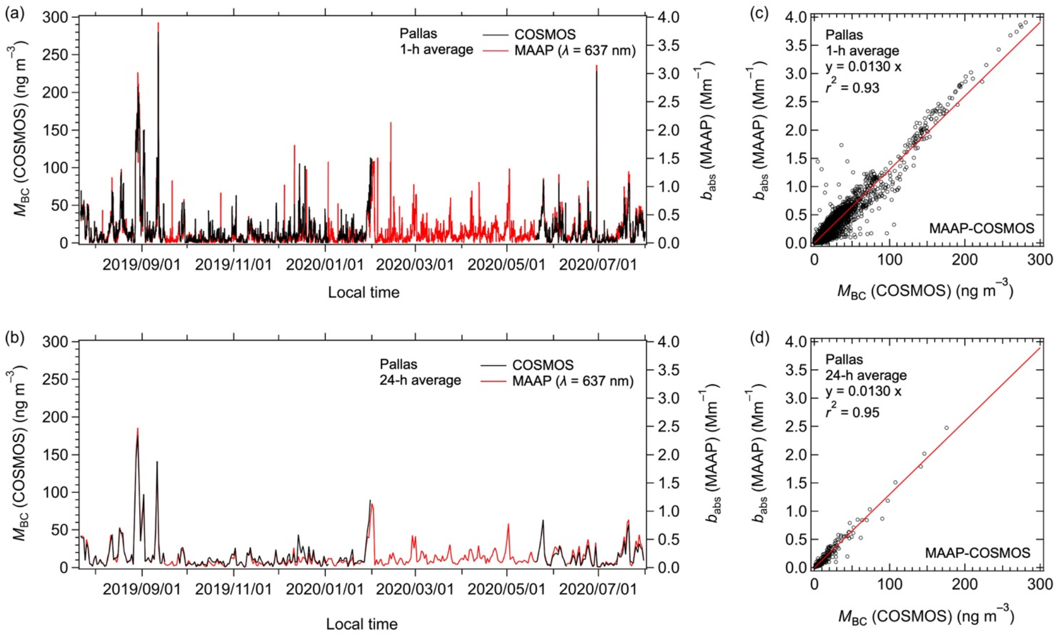


795 **Fig. 8.** Time series from July 2019 to July 2020 at Pallas of (a) 1-h averaged and (b) 24-h averaged $M_{BC}$ (COSMOS) and $b_{abs}$ (MAAP). (c) and (d) Corresponding correlations of $M_{BC}$ (COSMOS) and $b_{abs}$ (MAAP).

https://doi.org/10.5194/acp-2020-1190
Preprint. Discussion started: 11 December 2020


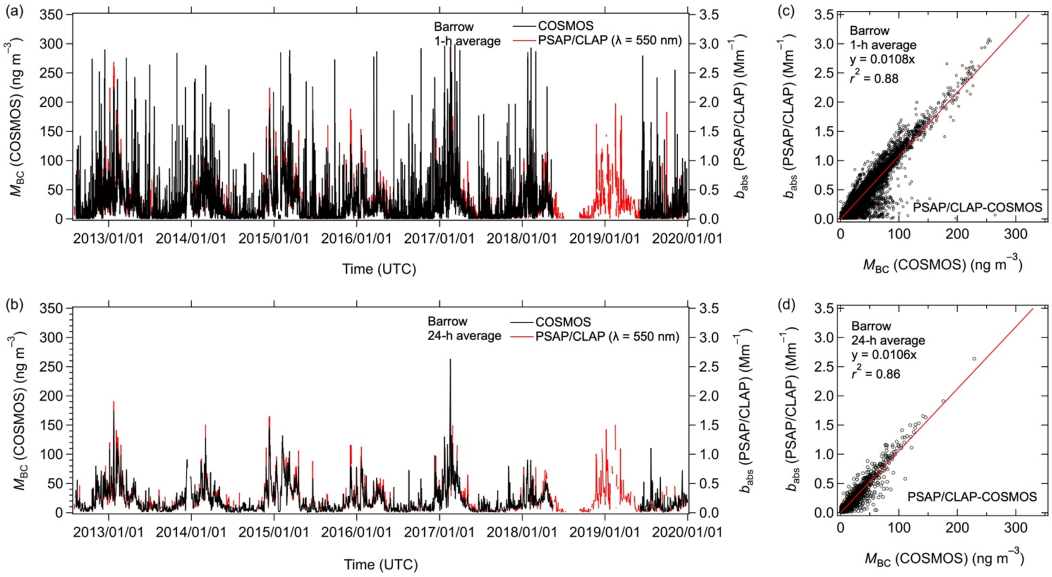


800 **Fig. 9.** Time series from August 2012 to December 2019 at Barrow of (a) 1-h averaged and (b) 24-h averaged $M_{BC}$ (COSMOS) and $b_{abs}$ (PSAP/CLAP). (c) and (d) Corresponding correlations of $M_{BC}$ (COSMOS) and $b_{abs}$ (PSAP/CLAP).

https://doi.org/10.5194/acp-2020-1190
Preprint. Discussion started: 11 December 2020


Atmospheric Chemistry and Physics Discussions

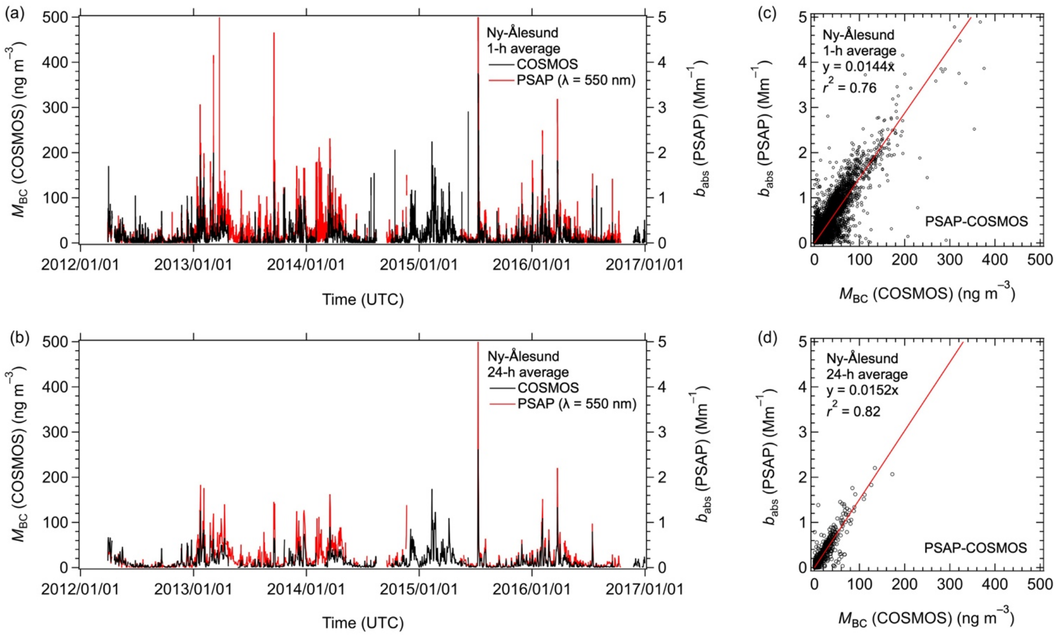


805

**Fig. 10.** Time series from April 2012 to September 2016 at Ny-Ålesund of (a) 1-h averaged and (b) 24-h averaged $M_{BC}$ (COSMOS) and $b_{abs}$ (PSAP). (c) and (d) Corresponding correlations of $M_{BC}$ (COSMOS) and $b_{abs}$ (PSAP).

810

https://doi.org/10.5194/acp-2020-1190
Preprint. Discussion started: 11 December 2020


Atmospheric Chemistry and Physics
Discussions

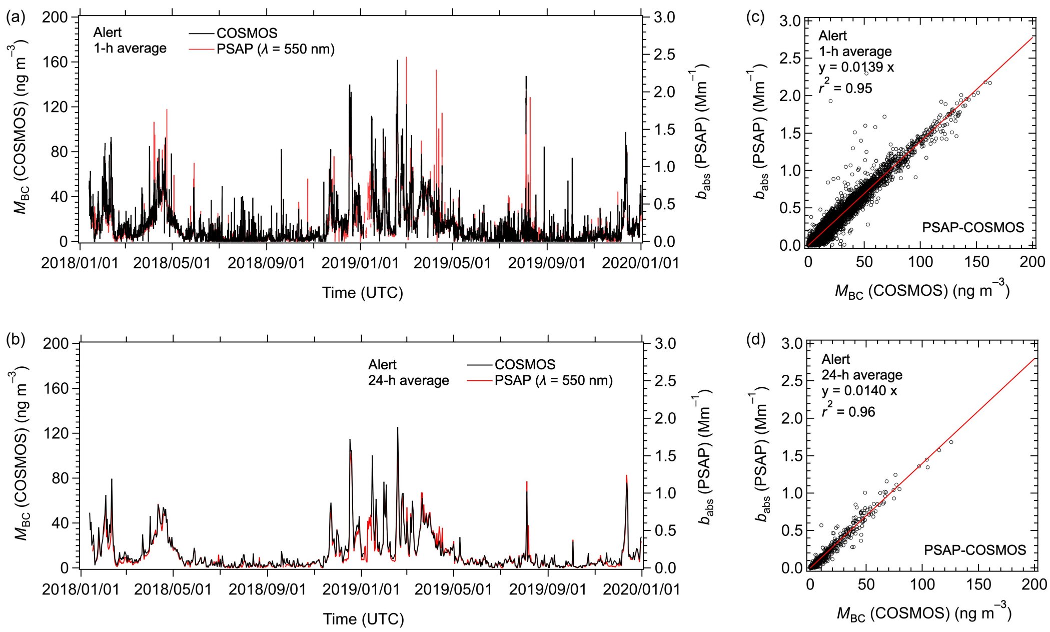


**Fig. 11.** Time series from January 2018 to December 2019 at Alert of (a) 1-h averaged and (b) 24-h averaged $M_{BC}$ (COSMOS) and $b_{abs}$ (PSAP). (c) and (d) Corresponding correlations of $M_{BC}$ (COSMOS) and $b_{abs}$ (PSAP).

815

https://doi.org/10.5194/acp-2020-1190
Preprint. Discussion started: 11 December 2020


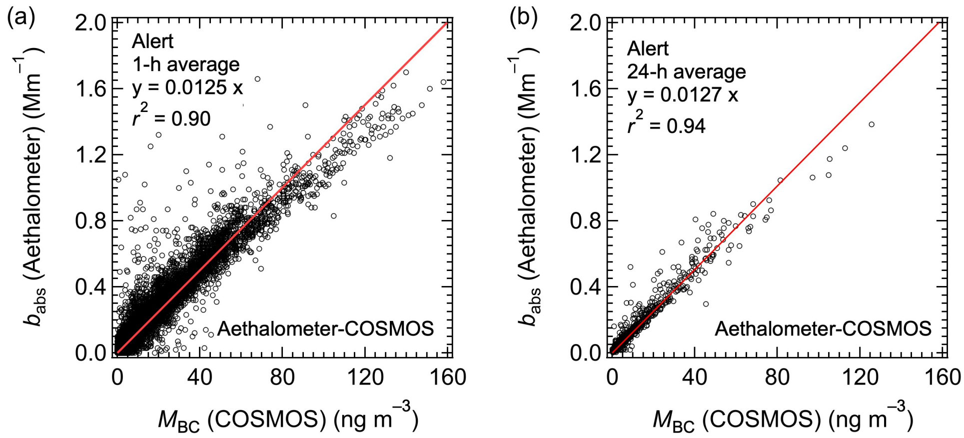


**Fig. 12.** (a) Correlations of (a) 1-h averaged and (b) 24-h averaged $M_{BC}$ (COSMOS) with $b_{abs}$ (Aethalometer) at Alert from January 2018 to December 2019.

820

https://doi.org/10.5194/acp-2020-1190
Preprint. Discussion started: 11 December 2020

Atmospheric Chemistry and Physics Discussions

## Tables

**Table 1.** Year-to-year variability of MAC (MAAP; λ = 639 nm) at Fukue.

| Year | MAC (1-h) [$m^2\ g^{-1}$] | $r^2$ (1-h) | MAC (24-h) [$m^2\ g^{-1}$] | $r^2$ (24-h) |
|---|---|---|---|---|
| 2009 (Apr–Dec) | 10.4 | 0.98 | 10.5 | 0.99 |
| 2010 | 9.62 | 0.95 | 9.74 | 0.95 |
| 2011 | 11.2 | 0.95 | 11.3 | 0.96 |
| 2012 | 12.6 | 0.96 | 12.7 | 0.96 |
| 2013 | 12.8 | 0.94 | 12.7 | 0.94 |
| 2014 | 10.7 | 0.98 | 10.8 | 0.98 |
| 2015 | 10.0 | 0.96 | 9.96 | 0.95 |
| 2016 | 9.90 | 0.95 | 9.97 | 0.95 |
| 2017 | 10.9 | 0.93 | 11.1 | 0.90 |
| 2018 | 11.4 | 0.96 | 11.5 | 0.96 |
| 2019 (Jan–May) | 12.1 | 0.95 | 12.2 | 0.95 |
| Average* | 11.1 ± 1.1 | 0.96 ± 0.02 | 11.1 ± 1.1 | 0.95 ± 0.02 |
| All** | 10.8 | 0.95 | 10.9 | 0.94 |

*Average for individual years
**Derived by correlation of all data points

**Table 2.** Values of MAC (MAAP; λ ~637 nm) recommended by instrument manufacturers and determined in this study.

| Location | Inlet | Period | MAC (1-h) [$m^2\ g^{-1}$] | $r^2$(1-h) | MAC (24-h) [$m^2\ g^{-1}$] | $r^2$(24-h) |
|---|---|---|---|---|---|---|
| Manufacturer | NA | NA | 6.6 | NA | 6.6 | NA |
| Fukue | $PM_1$* | 2009–2019 | 11.1 ± 1.1 | 0.96 ± 0.02 | 11.1 ± 1.1 | 0.95 ± 0.02 |
| Pallas | $PM_{10}$ | 2019–2020 | 13.0 | 0.93 | 13.0 | 0.95 |
| Average | | | 12.1 ± 1.3 | 0.95 ± 0.02 | 12.1 ± 1.3 | 0.95 |

*A PM2.5 cyclone was used before November 2011.

https://doi.org/10.5194/acp-2020-1190
Preprint. Discussion started: 11 December 2020



**Table 3.** Year-to-year variability of MAC (PSAP/CLAP; λ = 550 nm) at Barrow.

| Year | MAC (1-h) [m$^2$ g$^{-1}$] | $r^2$ (1-h) | MAC (24-h) [m$^2$ g$^{-1}$] | $r^2$ (24-h) |
|---|---|---|---|---|
| 2012 (Aug–Dec) | 9.00 | 0.65 | 8.80 | 0.67 |
| 2013 | 10.5 | 0.91 | 10.5 | 0.91 |
| 2014 | 11.0 | 0.96 | 10.8 | 0.91 |
| 2015 | 11.7 | 0.91 | 11.5 | 0.91 |
| 2016 | 11.3 | 0.89 | 11.2 | 0.88 |
| 2017 | 11.5 | 0.91 | 11.3 | 0.93 |
| 2018 (Jan–May) | 12.0 | 0.86 | 10.9 | 0.69 |
| 2019 (Jun–Dec) | 4.6 | 0.28 | 5.1 | 0.41 |
| Average (2012–2018)* | 11.0 ± 1.0 | 0.87 ± 0.10 | 10.7 ± 0.9 | 0.84 ± 0.11 |
| All** | 10.8 | 0.88 | 10.6 | 0.86 |

*Average for individual years
**Derived by correlation of all data points

**Table 4.** Year-to-year variability of MAC (PSAP; λ = 550 nm) at Ny-Ålesund.

| Year | MAC (1-h) [m$^2$ g$^{-1}$] | $r^2$ (1-h) | MAC (24-h) [m$^2$ g$^{-1}$] | $r^2$ (24-h) |
|---|---|---|---|---|
| 2012 (Apr–Dec) | 5.7 | 0.30 | 5.8 | 0.44 |
| 2013 | 17.0 | 0.81 | 17.2 | 0.85 |
| 2014 | 17.4 | 0.80 | 18.5 | 0.81 |
| 2015 | 12.0 | 0.84 | 15.9 | 0.94 |
| 2016 (Jan–Sep) | 14.5 | 0.90 | 14.8 | 0.95 |
| Average (2013–2016)* | 15.2 ± 2.5 | 0.84 ± 0.05 | 16.6 ± 1.6 | 0.89 ± 0.07 |
| All** | 14.4 | 0.76 | 15.2 | 0.82 |

*Average for individual years
**Derived by correlation of all data points

https://doi.org/10.5194/acp-2020-1190
Preprint. Discussion started: 11 December 2020

Atmospheric Chemistry and Physics Discussions

**Table 5.** MAC (PSAP/CLAP; λ) values at Alert during 2018–2019.

| Instrument | λ (nm) | MAC (1-h) [m$^2$ g$^{-1}$] | $r^2$(1-h) | MAC (24-h) [m$^2$ g$^{-1}$] | $r^2$ (24-h) |
|---|---|---|---|---|---|
| CLAP1 | 450 | 13.6 | 0.93 | 13.6 | 0.95 |
| CLAP2 | 450 | 15.4 | 0.96 | 15.4 | 0.96 |
| PSAP | 450 | 15.7 | 0.95 | 15.4 | 0.96 |
| CLAP1 | 550 | 12.1 | 0.93 | 12.1 | 0.95 |
| CLAP2 | 550 | 13.6 | 0.96 | 13.8 | 0.95 |
| PSAP | 550 | 13.9 | 0.96 | 14.0 | 0.95 |
| CLAP1 | 700 | 9.7 | 0.93 | 9.7 | 0.95 |
| CLAP2 | 700 | 10.8 | 0.95 | 10.9 | 0.95 |
| PSAP | 700 | 11.5 | 0.94 | 11.6 | 0.95 |

**Table 6.** MAC (PSAP; λ = 550 nm) values at Alert.

| Year | MAC (1-h) [m$^2$ g$^{-1}$] | $r^2$(1-h) | MAC (24-h) [m$^2$ g$^{-1}$] | $r^2$ (24-h) |
|---|---|---|---|---|
| 2018 | 13.5 | 0.96 | 13.3 | 0.97 |
| 2019 | 14.3 | 0.95 | 14.6 | 0.95 |
| Average | 13.9 ± 0.6 | 0.96 ± 0.01 | 14.0 ± 0.9 | 0.96 ± 0.01 |
| All | 13.9 | 0.95 | 14.0 | 0.96 |

**Table 7.** MAC (PSAP; λ = 550 nm) values at the 3 Arctic sites.

| Location | Inlet | Period | MAC (1-h) [m$^2$ g$^{-1}$] | $r^2$(1-h) | MAC (24-h) [m$^2$ g$^{-1}$] | $r^2$ (24-h) |
|---|---|---|---|---|---|---|
| Barrow | $PM_1$ | 2012–2018 | 11.0 ± 1.0 | 0.87 ± 0.10 | 10.7 ± 0.9 | 0.84 ± 0.11 |
| Ny-Ålesund | $PM_{10}$ | 2013–2016 | 15.2 ± 2.5 | 0.84 ± 0.05 | 16.6 ± 1.6 | 0.89 ± 0.07 |
| Alert | $PM_1$ | 2018–2019 | 13.9 ± 0.6 | 0.96 ± 0.01 | 14.0 ± 0.9 | 0.96 ± 0.01 |
| Average | | | 13.4 ± 2.2 | 0.89 ± 0.06 | 13.8 ± 3.0 | 0.90 ± 0.06 |

**Table 8.** MAC (Aethalometer; λ) values at Alert during 2018–2019.

| λ (nm) | MAC (1-h) [m$^2$ g$^{-1}$] | $r^2$(1-h) | MAC (24-h) [m$^2$ g$^{-1}$] | $r^2$ (24-h) |
|---|---|---|---|---|
| 370 | 18.6 | 0.86 | 18.7 | 0.90 |
| 470 | 15.4 | 0.89 | 15.6 | 0.93 |
| 520 | 13.9 | 0.90 | 14.1 | 0.94 |
| 590 | 12.5 | 0.90 | 12.7 | 0.94 |
| 660 | 11.4 | 0.89 | 11.6 | 0.94 |
| 880 | 8.8 | 0.82 | 8.9 | 0.94 |
| 950 | 8.1 | 0.79 | 8.1 | 0.94 |

https://doi.org/10.5194/acp-2020-1190
Preprint. Discussion started: 11 December 2020

Atmospheric Chemistry and Physics Discussions
Open Access
EGU

**Table 9.** MAC (PSAP) and MAC (Aethalometer) values derived from 24-h averaged data at Alert during 2018–2019.

| λ (nm) PSAP/Aeth | MAC(PSAP) [$m^2\ g^{-1}$] | MAC(Aeth) [$m^2\ g^{-1}$] | MAC (Aeth)/MAC (PSAP) |
|---|---|---|---|
| 450/470 | 15.4 | 15.6 | 1.01 (1.06)[*] |
| 550/520 | 14.0 | 14.1 | 1.01 (0.95)[*] |
| 700/660 | 11.6 | 11.6 | 1.00 (0.94)[*] |

[*]MAC (Aethalometer) values measured at λ = 470, 520, and 660 nm were adjusted to those at λ = 450, 550, and 700 nm (wavelengths used for PSAP) by assuming an absorption Ångstrom exponent of 1.0.

**Table 10.** MAC and $r^2$ of MAAP, PSAP/CLAP, and Aethalometer at λ = 550 nm at observation sites in this study.

| Location | Instrument | Inlet | Period | MAC (1-h) [$m^2\ g^{-1}$] | $r^2$(1-h) | MAC (24-h) [$m^2\ g^{-1}$] | $r^2$(24-h) |
|---|---|---|---|---|---|---|---|
| Fukue | MAAP | $PM_1$[*] | 2009–2019 | 12.9[***] | 0.96 | 12.9[***] | 0.95 |
| Pallas | MAAP | $PM_{10}$ | 2019–2020 | 15.1[***] | 0.93 | 15.1[***] | 0.95 |
| Barrow | PSAP/CLAP | $PM_1$ | 2012–2018 | 11.0 | 0.87 | 10.7 | 0.84 |
| Ny-Ålesund | PSAP | $PM_{10}$ | 2013–2016 | 15.2 | 0.84 | 16.6 | 0.89 |
| Alert | PSAP | $PM_1$ | 2018–2019 | 13.9 | 0.96 | 14.0 | 0.96 |
| Alert | Aethalometer | TSP[**] | 2018–2019 | 13.4[***] | 0.89 | 13.3[***] | 0.92 |
| Average in the 4 Arctic sites[****] | | | | 13.8±2.0 | 0.90±0.05 | 14.1±2.5 | 0.91±0.06 |

[*]A PM2.5 cyclone was used before November 2011.
[**]Total suspended particle.
[**]MAC (MAAP; λ ~637 nm) and MAC (Aethalometer; λ = 520 nm) values were adjusted to those at λ = 550 nm by assuming an absorption Ångstrom exponent of 1.0.
[***]Average values were calculated except for MAAP data at Fukue and Aethalometer data at Alert.